5-7-2011

Finite Element Analysis of the Effect of Low-Speed Rear End Collisions on the Medial Meniscus

Daniel J. Tichon
University of Connecticut - Storrs, daniel.tichon@uconn.edu

Finite Element Analysis of the Effect of Low-Speed Rear End Collisions on the Medial Meniscus

Daniel Joseph Tichon

B.S., University of Connecticut, 2010

A Thesis

Submitted in Partial Fulfillment of the

Requirements for the Degree of

Master of Science

at the

University of Connecticut

2011

APPROVAL PAGE

Master of Science Thesis

Finite Element Analysis of the Effect of Low-Speed Rear End Collisions on the Medial Meniscus

Presented by

Daniel Joseph Tichon, B.S.

Major Advisor _____
Dr. Donald Peterson

Associate Advisor _____
Dr. John Bennett

Associate Advisor _____
Dr. Wei Sun

University of Connecticut

2011

ACKNOWLEDGEMENT

D.J.T. sincerely appreciates the constant guidance and support of Dr. Peterson throughout the research and writing of this thesis. D.J.T. would also like to thank Dr. Sun and Dr. Bennett for their suggestions and contributions to this thesis. D.J.T. thanks Technology Associates of Stamford, CT for the original research concept and feedback throughout the project.

TABLE OF CONTENTS

LIST OF TABLES

LIST OF FIGURES

ABSTRACT

Low-speed, rear end vehicle collisions can inflict soft tissue damage to the passenger's knees, especially the medial meniscus, which has been previously unexplained in published literature. It is difficult to determine if factors such as age or other injury was the primary cause of the injury or if the accident acutely caused the meniscal tear. Rear end collisions may produce a combination of compressive loading and torque about the knee that will injure the medial meniscus during the initial impact and the rebound phase. The purpose of this study is to determine if it is possible for rear end low-speed collisions to tear the medial meniscus when the knee had no significant contact with the interior of the vehicle.

A three-dimensional finite element model of the knee was used to determine the effect of various loads and torques imposed on the knee using the software FEBio. Compressive loading, knee flexion, axial torque, and varus torque were applied to the knee through the femur, and the stress and strain within the medial meniscus were determined. It was found that increased knee flexion along with compressive loading will increase the stress observed as compared to the knee in the neutral position. Axial torque up to 24 Nm and varus torque will both increase the stress observed in the meniscus. In a collision, if the knee experiences any type of axial or varus torque coupled with a compressive force of 670 N or more, there is a possibility that the medial meniscus will be torn. It was also found that the areas of maximum stress occur along the inner edge of the meniscus and are found primarily in the mid-body and posterior horn. While there are several inherent limitations of the current model, the results of the simulations show that several loading patterns can stress the medial meniscus to failure, especially if it was in a weakened state due to mechanical trauma or age.

1. Introduction

Rear end motor vehicle collisions that occur at low speed may produce forces large enough in magnitude to cause soft tissue injury, especially in the neck and knee regions. Whiplash is the most common injury claimed from rear end collisions but there is a significant population that claims to injure their knee, particularly the medial meniscus. It is often difficult to determine if the knee injury was caused solely by the accident or if previous other factors such as previous injury or age actually played a larger role in the injury. Since there is limited published research pertaining to injuring the medial meniscus, finite element analysis will be used to model forces imposed upon the knee to gain a greater knowledge of meniscal injury mechanisms. In this thesis, a three-dimensional computer automated design (CAD) model of the knee, complete with the medial meniscus and surrounding ligaments, was used to test various loading conditions that might be found in a rear end vehicle crash. The purpose of this study was to determine if it is possible for non-contact loading mechanisms, such as that may be seen during a rear end collision without significant contact with the interior of the vehicle, to tear the medial meniscus using a finite element approach.

1.1 Low-Speed, Rear End Collisions

A low-speed, rear end collision generally involves two vehicles and takes place when both vehicles are moving less than fifteen miles per hour as the bullet vehicle strike the target vehicle from behind. In many of the cases analyzed, the target vehicle was either stopped, slowing to a stop, or slowly accelerating when the bullet vehicle struck it from the rear, such as is illustrated in Figure 1. These accidents often occur at traffic

lights or in stop-and-go traffic where the driver of the bullet vehicle did not see the other vehicle or was unable to stop in time. The driver or passenger in the target vehicle is almost always the plaintiff in rear end collision cases, which may be due to the exposure to larger forces. Rear end collisions are generally aligned front-to-back, but there is the possibility for the collision to occur at an oblique angle, which is shown in Figure 1c.

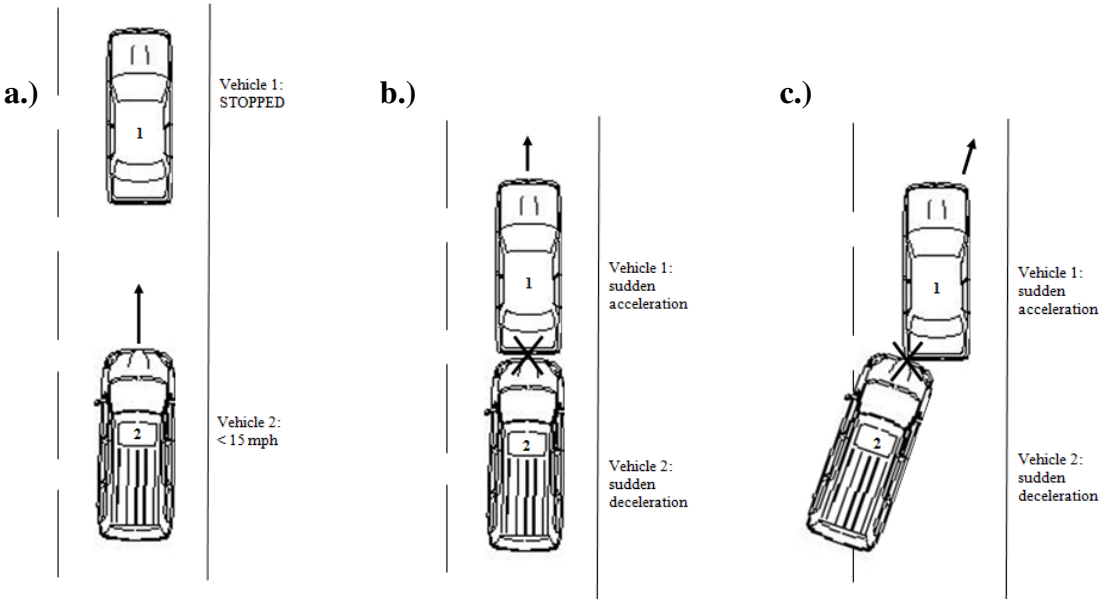

Figure 1: Low-speed rear end collision is composed of a target and bullet vehicle (a.), and an impact that accelerates the target vehicle forwards (b.) or sideways (c.)

Upon inspection, low-speed collisions usually have little-to-no structural damage to either vehicle, since the bumper and frame are able to rebound back to its original shape without being permanently deformed. The speed is also low enough that the airbags do not deploy and other emergency sensors may not be tripped within the vehicles. It is from these observations that many people mistakenly assume that no serious injury can be inflicted in such accidents but sufficient forces are present that may injure several parts of the body. Whiplash is the most common injury reported since even small accelerations transferred to the bullet vehicle can be magnified when the neck

snaps forwards and backwards against the headrest within a small amount of time. The inertial forces associated with the relatively heavy head attached to a flexible neck are able to greatly exceed safe limits, injuring the ligaments, disks, and even vertebrae within the neck. Often, a secondary injury that is reported along with whiplash is a knee injury, which may include injury to any of the soft tissues within the knee capsule. In particular, there are a large amount of injuries that affect the medial meniscus in either the left or right knee.

Several factors may influence the severity of a low speed collision and the likelihood of soft tissue injuries. A greater change in velocity increases the acceleration that the body experiences and thus affects the magnitude of the forces. The weight of the vehicles involved plays a role in the forces transmitted between the vehicles and, therefore, within the knee. A larger bullet vehicle such as a truck or heavy van has a much larger mass than a normal passenger car and would impart a larger force to the target vehicle. This can also work the other way around, with a larger target vehicle being safer since a smaller vehicle would need to be traveling at much greater speeds to impart the same magnitude of force to the target vehicle. Internal factors such as seatbelts, seat back angle, and lower body position all play a role in the dynamics of a person in a vehicle that is struck by another vehicle in the rear.

There are several types of knee injuries that may occur as a result of inertial forces or the interaction of the knee within the vehicle. If the knee contacts an inner surface of the vehicle with significant force, the collision may result in patellar, femoral, or tibial fractures. Knee contact with a solid object such as the dashboard or center console can also dislodge the tibia far enough in relation to the femur that the ligaments

are stressed to their breaking points. Non-contact injuries may include ligament tears, such as the ACL and MCL, and tears in the cartilage and menisci. This study will focus on medial meniscal tears caused by non-contact mechanisms of injury (i.e., no significant contact with the interior of the vehicle) as there is no published data on the cause of such injuries and little is known as to why these tears occur. This study will explore possible ways that the meniscus can be torn so that future studies can relate this information to the biomechanics of rear end car crashes.

1.2 Meniscal Tear Statistics

In general, there are 850,000 meniscal tear surgeries performed annually in the United States, encompassing all types of injuries including sports, vehicle accidents, and degenerative tears. For general meniscal injury, the peak age of incidence for white males is 31 to 40 years and is 11 to 20 years for females. After the age of 65, 60% of all adults have degenerative meniscal tears (WebMD, 2009). In one study, 88% of the subjects tore their medial meniscus while doing various activities, while only 12% tore their lateral meniscus (Shakespeare, Rigby, 1983). Since the majority of meniscal tears occur in the medial compartment of the knee, this type of injury is the focus of this study. They also found that 40% of these tears occurred during a simple twist, 36% occurred while playing sports and 2% occurred during road traffic accidents.

According to Jury Verdict Review and Analysis, 40,728 civil cases have gone to trial for motor vehicle negligence since 1980 and 29% of these cases involved rear end collisions, where 6.2% of the rear end collision cases had a complaint of knee injury and 25% complained of a meniscal tear (JVR&A, 2010). According to this sampling, 2% of

all rear end collisions result in a meniscal tear, which is a small but significant percentage of people that sustain meniscal injuries during rear end collisions. Assuming 850,000 meniscal tears occur each year in the United States, this equates to approximately 5000 medial meniscal tears that occur during rear end collisions. A full breakdown of the percentages of knee injuries reported online and some details of these collisions can be found in Appendix A.1 and A.2. It is important to understand why these injuries are occurring, so that it may be possible to reduce the amount of knee injuries by improving safety features within vehicles or instructing drivers on the proper way to sit in their seats.

1.3 Knee Anatomy

The knee is one of the most complex joints in the human body due to the variety of ligaments, cartilages, bones, and degrees of freedom involved with its movement. The femur is attached to the tibia through the Medial and Lateral Collateral Ligaments (MCL and LCL) and the Anterior and Posterior Cruciate Ligaments (ACL and PCL). Articular cartilage covers the surface of the bones and the medial and lateral menisci serve as shock absorbers in between the femur and tibia, which can be seen in Figure 2. The periphery of the menisci is attached to the tibia by the coronary ligaments but the inner edges are free to move. The knee also includes the tendons that attach the quadriceps and hamstring muscles to the bones and hold the patella in place. Bursae are small fluid filled sacs that are found by the patella in the front of the knee to decrease friction during flexion. In addition to the complexity of the structural members, the knee undergoes several degrees of freedom during the knee bending motion. During normal gait, the

knee will flex and extend but the tibia also rotates with respect to the femur in a fashion similar to a screw mechanism. This non-planar movement aids in the efficiency of locomotion and is a function of the complex structure of the knee joint but it also makes it difficult to model the full range of motion (Peterson, Bronzino, 2008).

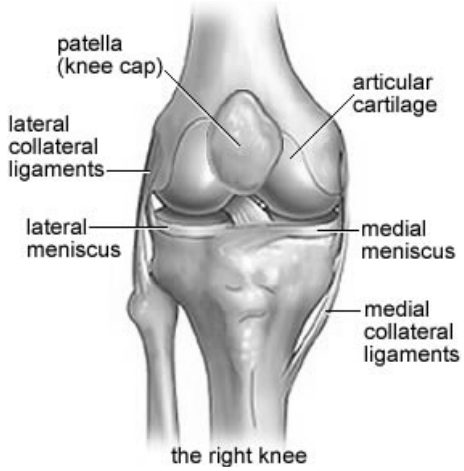

Figure 2: Anatomy of the Knee (Anatomy of the Knee, 2001)

The menisci are C-shaped cups that are composed of fibrocartilage with horizontal layers of fibers oriented in alternating directions. Fibers oriented in the axial, longitudinal, and circumferential directions within the meniscus give it tensile strength in several different directions. Both the lateral and medial menisci are attached to the proximal end of the tibia but also conform to the distal end of the femur, providing an extremely low friction interface between the upper and lower leg during movement. The majority of the meniscus is avascular, meaning that the lack of constant blood supply makes it very difficult for the meniscus to heal if it is damaged. Tears can result in a flap of the meniscus obstructing the normal movement of the knee while causing joint locking and pain of the knee. Meniscal tears generally affect the screw-home mechanism of the knee, which turns it into a planar joint instead of allowing the tibia to rotate laterally on the femur during the final stages of knee extension (Frankel et al., 1971). Often, the only

solution is to excise the damaged tissue but a full meniscectomy has been proven to accelerate osteoarthritis and other bone problems within the knee. Since the meniscus cannot regenerate and it is especially difficult to heal, it is beneficial to take steps to avoid meniscal injury to avoid having to deal with these difficulties.

1.4 Mechanism of Injury

Internal derangement of the knee is the disruption of the normal functioning of the knee ligaments or cartilage which can be caused by physical trauma (Bentley, G., 1996). Any trauma in the form of a valgus force or axial torque about the knee is able to severely tear or rupture the internal components of the knee joint. The medial collateral ligament is the most commonly injured part of the knee but it is closely followed by the medial meniscus and then the ACL. This could be due to the relative strengths of each structure and the loading patterns that increase the likelihood of injury during certain activities. Strength of the muscles surrounding the knee is also important to prevent injury since subjects with weaker legs may be more prone to injury (Bristow, W.R., 1925). It may prove beneficial for people to perform strengthening exercises for their leg muscles if they consistently do activities that may increase the risk of knee injury.

Meniscal tears generally occur due to specific loading conditions that stress the meniscus to the point of failure. Meniscal tears can be caused from a rotational stress applied to a flexed knee under compression loading or by the femur moving too far forwards or backwards in relation to the tibia (Bentley, W.R., 1996). When the tibia is internally rotated while the knee is flexed, the posterior horn of the medial meniscus is pulled towards the center of the joint and this can create a tear (Solomen et al., 2001).

Compression of the knee can trap a portion of the meniscus while another portion moves and this creates tension that leads to a tear if the applied force is greater than the material strength. A traction injury that stretches the leg can also cause a tear of the peripheral attachments and may produce a longitudinal tear of the meniscus (Solomen et al., 2001). Although the meniscus is attached to the tibia, but not directly to the femur, the edge of the meniscus is attached to ligaments that also connect the tibia and femur together. A tension force in these ligaments would pull the edge of the medial meniscus, creating a force that may lead to a tear if it is of sufficient magnitude. If either of the tibia or femur moves to a significant degree in coronal or saggital planes, a tensile force will be applied to the MCL and LCL and can be transmitted to the medial meniscus. Another cause of meniscus injury is degeneration associated with age that will diminish the strength and flexibility of the meniscus in people over the age of 50. Aging causes a delamination of the meniscus that can result in horizontal tears in the presence of shear stress (Solomen et al., 2001).

The meniscus is more commonly torn while playing sports since there is a greater amount of torque and force applied to the leg than ordinary tasks. For example, a 150 lb. person skiing at 30 mph can apply 15 G, or 2250 lbs., of force to their knees as they stop (Erskine, L.A., 1950). The incidence of injury was also seen to increase as fatigue of the skier increased, supporting the fact that muscle strength and reaction time is important to prevent injury. It is common for a person to plant their foot firmly on the ground while having a flexed leg and then to rotate their upper leg and body, such as might be seen in soccer or football while cutting and running in different directions. The combination of applying a compressive load and twisting the femur is perfect for tearing the medial

meniscus and, unfortunately, there are a number of activities that may involve these conditions. The purpose of this research is to determine if it is possible for a low speed collision to produce the forces necessary to replicate the damage often seen in sports injuries.

The most common types of meniscal tear are oblique and transverse tears that occur in the posterior horn and originate from the inner edge (Fan, R.S.P., Ryu, R.K.N., 2000). This occurs due to the fact that the periphery and posterior horn of the meniscus are fixed to the tibia while the inner edge is free to move (Bristow, W, 1925). The extra freedom of movement can be a hazard because if the meniscus moves a great enough distance, there is a greater tensile force applied within the body of the meniscus. A longitudinal tear is a common tear that occurs along the length of the meniscus, while a horizontal tear separates the layers of the meniscus (Fan, R.S.P., Ryu, R.K.N., 2000). The thinnest section of the medial meniscus is the inner edge, where it tapers to a thin edge, and is the area where most tears originate. Figure 3 illustrates the most common tears that occur during meniscal injuries.

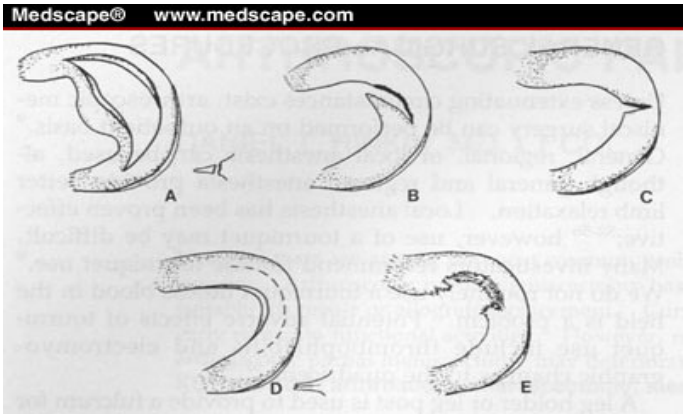

Figure 3: Common Types of Meniscal Tears (A- Longitudinal Tear, B- Oblique Tear, C- Transverse Tear, D- Horizontal Tear, E- Complex Degenerative Tear)
(Erskine, L.A., 1950)

According to current research, medial meniscal tears are most common in men with the average age being 29 years old (Shakespeare, Rigby, 1983). The meniscus can be injured by a simple twist, by playing sports, crouching, a valgus force to the knee, a transverse movement of the tibia, or any activity that places compression on the knee while rotating and flexing it (Bentley, G, 1996). Any force that compresses the meniscus so that it becomes trapped on one end has the potential to cause injury.

1.5 Knee Dimensions and Material Characteristics

To date, no published data could be found on the cause of meniscal tears in low speed, rear end motor vehicle collisions. There are a few references that discuss the material properties and dimensions of the medial meniscus and these formed the basis of the preliminary research on knee injuries in rear end collisions.

Several papers used radiographs, MRI images, and autopsies to determine the dimensional relationships of the menisci within the knee. Haut et al. (2000) used a three dimensional coordinate digitizing system along with MRI to find the geometry of the menisci in several subjects. Stone et al. (2007) attempted to determine if there was a relationship that would be able to predict the size of the meniscus based on gender, height, and weight but were unable to find a suitable relationship. These papers give an idea of the approximate size of the medial meniscus and were used in the initial analysis of its structure and function for this research. A simple medial meniscus model could be created using the average dimensions published in these papers but they are unable to accurately describe the complete geometry. These papers show that every subject has slightly different size menisci and it is very difficult to predict the exact dimensions for a

certain person without using some type of imaging. A complete set of values for these dimensions from these publications have been included in Appendix B.

The material characteristics of various parts of the knee were described in several articles and were used to get a complete understanding of how the knee reacts under loading. Another study described the biomechanical aspects of cartilage, which included the composition, structure, and mechanical behavior (Mansour, J.M., 2009). Phisitkul et al. (2006) described the anatomy, biomechanics, and strengths of the Medial Collateral Ligament while Mathur et al. (1949) gave measurements on different types of fractures often seen in menisci. One study found the average tensile strengths for different areas within the meniscus and it showed that the strengths varied with the orientation of the fibers within the meniscus (Bullough, P.G., et al., 1970). Kennedy et al. (1976) found the tibial collateral ligaments, PCL and ACL yield points and ultimate failure strengths with the PCL being the strongest ligament tested. These articles describe the individual strengths of the components within the knee capsule and can help to get a better representation of the strength of the entire knee. The knee will fail at its weakest point for a certain loading geometry and the individual ligaments and cartilages can be tested to determine what would be most likely to fail first. Research supports the findings that certain structures such at the ACL and meniscus are prone to rupture during activities that put undue stress on them. In order to model a full knee in finite element software, the material properties for each structure is needed, and these articles provide a basis for these values.

For testing on a full scale, cadaver models have shown that an axially loaded tibia bent at 120 degrees of flexion can cause both ACL and meniscal tears. During the same

tests, the knee was shown to fail at approximately 4.4 kN of force applied to the tibia with the average medial meniscal pressure being 19.3 MPa (Jayaraman et al., 2001). Ex-vivo testing of the meniscus alone has shown that the tensile strength is dependent on the orientation of the fibers since they are the primary structure designed to resist tension in the meniscus. Interestingly, there was an increase in tensile strength as age increased that could be explained by an increase in cross linking between the fibers that is seen more prominently in older subjects (Bullough, P.G., et al., 1970). At the same time, excessive age may serve to weaken the meniscus due to the degradation caused by constant use and the inability for the meniscus to repair itself. While these articles are an excellent starting point to gain a more complete understanding of the mechanics of the materials within the knee, there are a few shortcomings associated with relying solely on this data. Ex-vivo testing of individual knee structures does not give a complete picture of the loading patterns that would be seen in a complete knee. Cadaver testing is more accurate since it involves the entire knee but the material properties of the tissue may be slightly altered due to the preservation techniques used after the subject's death. A computer-based finite element model of the entire knee could be an acceptable alternative but requires the material properties and boundary conditions to be known for each section of the model.

1.6 Finite Element Models

Although several knee models previously created in various finite element software programs are not freely distributed, they provide some crucial parameters that can be used for future models. Pena et al. (2005) modeled the menisci as single-phase, linear elastic, and isotropic material with a Young's Modulus of 59 MPa. They assumed

frictionless contact for all contact surfaces and found that the menisci transfers 81% of the total axial load during walking, with the medial menisci transferring 49% of that load. Another model was created that used a linearly elastic, transversely isotropic representation with different Young's Moduli for the axial and circumferential directions (Donahue. et al., 2004). They used 8 node trilinear hexahedral units in a "hard" contact model that allowed for no penetration of one surface into another. The shear moduli, horn stiffness, and stiffness of attachment sites were evaluated and included in their research as well. A separate group modeled a composite isotropic matrix reinforced by collagen fibers with an Elastic Modulus of 60 MPa and a tensile elastic modulus of 170 MPa (Bendjaballah et al., 1995; 1997). Each paper used slightly different parameters that were based on their own research or testing and provide a point for comparison for the current finite element analysis of the knee. The model parameters compared in Table 1 were used to create various finite element models suitable for analyzing the reaction in the knee during a rear end collision.

Table 1: Summary of Published Finite Element Model Parameters

Reference	**Description**	**E_{ax}/E_{cir} (MPa)**	**Poisson's Ratio (v)**	**Shear modulus (MPa)**
18	Single-phase linear elastic isotropic	59	0.49	~
19	Linearly elastic, transversely isotropic	20, 150	0.2, 0.3	57.7
25	Linearly elastic, transversely isotropic	20, 140	0.2, 0.3	~
20	Transversely isotropic	20, 150	0.2, 0.3	57.7
21	Composite isotropic matrix with fibers	8, 70, 50	0.45	~

1.7 Published Meniscal Strengths

There are few resources that have determined the exact strengths of the menisci in humans and no literature to date has been found detailing the strength of the meniscus under a combination of compression, torque, and flexion. Bullough et al. (1970) attempted to determine the tensile characteristics of the medial meniscus by cutting 9-20 μ thick sections from various sections. It is thought that the meniscus will most likely fail in tension due to traction seen within the knee joint during certain loading conditions. The orientations of the collagen fibers within the meniscal specimen were determined using polarized light microscopy and then tensile tests were performed using a specially designed tensometer. The tensile strength of the medial meniscal specimen depended heavily on the orientation of the fibers, with the greatest strength being observed with the fibers parallel to the applied uniaxial tensile force. With the fibers perpendicular to the applied force, the minimum tensile force observed was 0.448 MPa but the maximum tensile strength was 9.307 MPa with the fibers in an oblique position and with cross fibers. The testing showed that a 42 year-old male with oblique and cross linking fibers had a tensile strength ranging from 0.855 to 1.062 MPa. A 60 year old female with oblique and cross linking fibers had a tensile strength ranging from 2.633 to 2.841 MPa. It was thought that an increase in age increases the fiber cross linking within the meniscus and thus increases the tensile strength, assuming there is no other mechanical degradation associated with age.

A second paper also determined the tensile strengths of the medial meniscus by excising 31 fresh frozen menisci from cadavers ranging from 29 to 45 years old (Tissakht, M., Ahmed, A.M., 1995). Slices were cut from the medial menisci in the axial

and circumferential directions and then uniaxial tensile testing was performed to determine their strengths. It was found that the average stresses and strains varied between the proximal, middle, and distal layers, as well as the between the posterior and central regions. The average maximum tensile stress of a radial sample was 2.66 MPa with a minimum of 1.57 MPa, and the strain ranged from 0.3347 to 0.4311. The maximum stress of the circumferential sample ranged from 15.10 to 16.21 MPa with the maximum strain ranging from 0.2717 to 0.2858. The average of these values was found to be 8.34 to 9.44 MPa for the maximum stress and 0.3032 to 0.3585 for the average strain. The results of the simulations discussed later can be compared to these values to determine when the medial meniscus will fail under loading.

1.8 Biomechanics of Rear End Collision

A qualitative analysis of a low speed, rear end collision was performed to get a better understanding of the biomechanics involved and how a force may be transmitted to the medial meniscus. During such a collision, the occupants of the target vehicle are more likely to sustain a knee injury, so an analysis of the motion of the subjects for the target vehicle is discussed in greater detail. A low speed collision is composed of an initial strike caused by the bullet vehicle traveling at a greater velocity than the target vehicle and then a rebound phase immediately following the impact, which is illustrated in Figure 1. During the collision, the occupant of the target vehicle initially moves backwards relative to the vehicle and then rebounds forwards, creating movement of the lower body and loading conditions that may be sufficient to injure several aspects of the knee joint. Figure 1c shows how the line action for the impact force can be offset if the

bullet vehicle does not strike the target vehicle squarely in the rear. This would create a larger amount of torque within the knee since there is an applied lateral aspect of the line of force instead of just a front-to-back motion. This could possibly increase the chances of meniscal injury but the majority of rear end collisions are of the type seen in Figure 1b.

Right before the initial impact, the occupants of the target vehicle are generally not braced unless they see the car coming or hear the squealing tires of the bullet vehicle. This means that their legs are in a comfortable position that allows for easy access to both the brake and gas pedal with their right foot and their knee is not locked or in an extended position. The driver may have their arm on the console or may be leaning sideways at the time of impact, affecting the direction of the impact force. The driver's foot is most likely on the brake pedal, since rear end collisions generally occur in low speed situations such as at a traffic light. According to studies, the duration of the impact is relatively short at only 77 to 134 ms long (Nordhoff, L.S., 2005). During this time, the bullet vehicle's bumper makes contact with the rear of the target vehicle, accelerating the target vehicle forwards. If the bullet vehicle has a center of gravity that is higher than the target's, the target vehicle will be accelerated forwards and downwards at the same time. According to the law of conservation of momentum, a bullet vehicle with a greater mass than the target vehicle will impart a higher departure velocity and thus a greater amount of force on the target vehicle. The accidents most likely to injure the knee would involve larger trucks or SUV type vehicles that weigh more than a typical passenger car and also have a greater vertical height. This also suggests that driving a larger vehicle may be safer for the occupants if they are struck by another vehicle since they would experience less acceleration and, therefore, less force applied to their body.

The target vehicle has reached 60% of its maximum speed at 50 ms after the initial impact and the driver moves backwards, compressing the seat cushions. At 60 ms, the compressed seat cushions move the driver's hips and low back forwards and upwards while the seatback is flexing upwards. At 100 ms, the seatback reaches its maximum rearward rotation of about 10 degrees, which is dependent on the driver's body mass. At the same time, the vehicles separate with an average restitution of 0.40, which describes the departure speed of the two vehicles immediately after the collision. At 110 to 120 ms, the driver's body will ramp, or slide, up the seatback and maximum head acceleration occurs. Low speed collisions do not produce enough force to break the seatback, so the body's motion is constrained by the seatbelt and the flexing seatback. At 170 ms, the motion of the trochanter will reverse from moving upwards to moving downwards due to the lap belt force. Generally, the occupant motion will continue for 200 to 400 ms after initial impact and will have a second peak acceleration at 220 ms of about 6 G. Seatbacks have been proven to produce a rebound velocity of 80% to 150% of the initial impact velocity, which increases the severity of the collision (Nordhoff, L.S., 2005). Figure 4 shows the motion of the driver during the first 500 ms after a rear end collision.

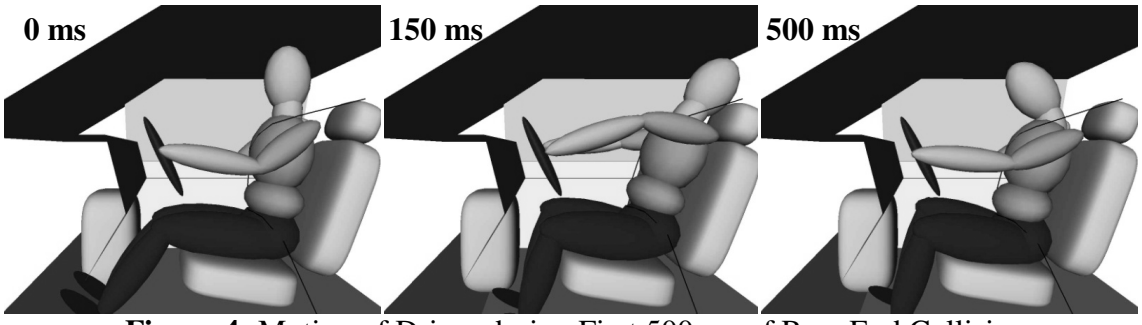

Figure 4: Motion of Driver during First 500 ms of Rear End Collision

With regards to the lower body, a driver may start with an upright and straight posture with the right foot on the brake and the knee either straight forward or slightly open. At the initial impact, the body moves rearward relative to the vehicle and the feet come off the foot pan while sliding backwards. The knees start to angle outwards with the knees farther apart and the foot angled outwards. There may also be contact with the calf and the front of the seat which could serve to disrupt the knee capsule by creating a shear force. During the rebound phase, the seat cushion pushes the body forward, relative to the vehicle, and the feet remain in position on the floor with the knees angled laterally outwards. The combination of the compressive force and twisting motion of the legs may create a situation that leads to injury.

In order to accurately model the loads transmitted to the menisci during a rear end collision, the knee flexion angle of the subject is required. This angle is dependent on the angle of the seat pan, the placement of the feet on the brakes or foot pan, and the height of the seat relative to the vehicle floor. Each vehicle has a slightly different seat configuration and the size of the subjects legs can impact the knee flexion angle, but a mean angle can be determined for an average size person for use in a finite element model. Vehicle test reports were downloaded for twenty-five common passenger vehicles from the National Highway Traffic Safety Administration (NHTSA) online database and these provided the body position of an average sized driver and passenger. The knee flexion angle was found by summing the values for the tibial angle and the pelvic angle specified in the NHTSA reports and these were seen to vary from approximately 56º to 88º (NHTSA, 2011). The median value for the knee flexion angle of the twenty-five passenger vehicles and light trucks was 71º while the mean value was

72º. The passenger knee flexion angles were consistently smaller than the driver's, but the difference was small enough that it was not significant. The average knee flexion angle of 72º will be used in the finite element model to simulate accurate loading conditions of a driver in the target vehicle.

1.9 Mechanisms of Injury in Rear End Collisions

The previously mentioned ways to injure the meniscus can be applied to the biomechanics of a subject inside a vehicle that experiences a rear end collision. Compression of the leg coupled with a torque has been proven to cause medial meniscal tears, something a rear end collision may be able to supply. During a rear end impact, the driver of the target vehicle rebounds off the seat and moves forwards with respect to the vehicle but their legs remain stationary on the floor due to friction. The forward velocity of the torso and the pelvis would load the flexed knee under compression which may be significant enough to pinch the meniscus. When the upper leg is not aligned straight with the vehicle prior to the impact, the leg would tend to move laterally due to the hinge effect about the hips. As the legs move laterally, an internal torque is applied to the knee joint and this combination of torque and compression along with the previously flexed knee may be sufficient to tear the meniscus. If the driver anticipates the impact by bracing themselves, the muscle tension of the legs will be increased, providing an added amount of compression within the knee. Other possible ways to injure the medial meniscus include applying a tensile load to the leg or from a direct impact to the knee from the inside of the vehicle, but these loading conditions may be more difficult to produce a tear in the meniscus. Figures 5 and 6 show some of the forces involved in a

rear end collision and illustrate how they act upon the lower body to create compression and torque.

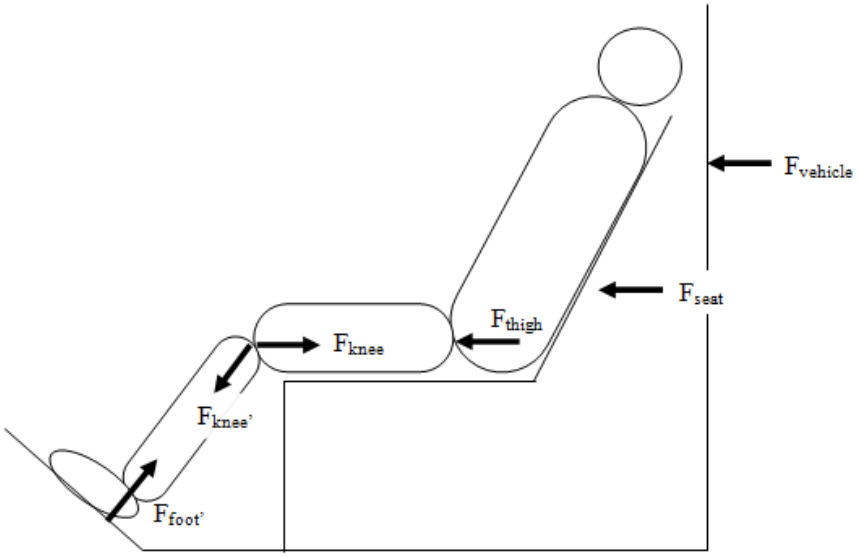

Figure 5: Side view of forces acting upon the lower leg in rear end collision

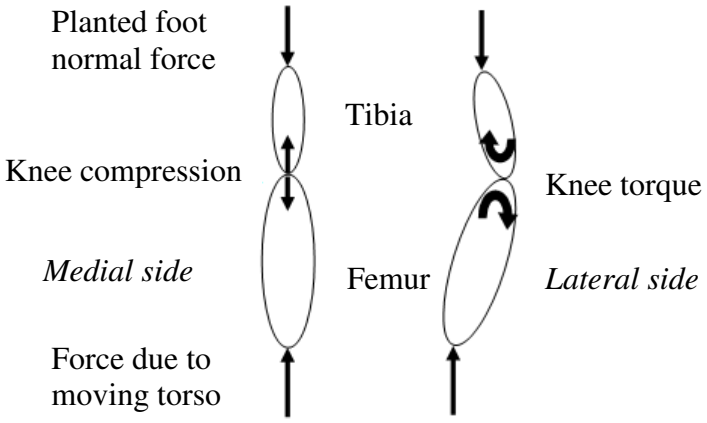

Figure 6: Top view of forces acting upon the femur and tibia in rear end collisions

In Figure 5 and 6, there is a force applied to the target vehicle ($F_{vehicle}$) that is equal to the mass of the bullet vehicle times the change in velocity that occurs during the collision. This force is transferred to the seat and can be magnified since the seat may behave like a spring, creating a larger force applied to the torso of the driver (F_{seat}). A

certain amount of this force is then transmitted to the femur (F_{thigh}), the knee (F_{knee}), and finally the foot which is planted on the floor of the vehicle (F_{foot}). If the knee remains in line, there will be pure compression of the knee while it is in the flexed position. If there is movement of the hips during the collision, or if the line of action of the impact is not completely front-to-back like in Figure 1c, the knee will move laterally and create an internal torque.

The majority of people who are involved in low speed, rear end collisions do not sustain knee injuries but a small population seems to have a knee injury inflicted upon them. This may be due to a larger change in vehicular velocity for the accident or a greater body mass of the subject, both of which would increase the magnitudes of the forces present in the knee. The size of the vehicles could significantly influence the severity of the collision and the initial body geometry of the people could affect the chance of injury. An increased strength of the ligaments and muscles surrounding the knee may also reduce the severity of an injury when the knee is affected by the external forces. People with degenerated menisci, commonly due to age or wear, would have a greater likelihood of knee injury and would require a much lower magnitude of force to tear the meniscus. Females have naturally weaker and smaller menisci, as compared to males, but also tend to have less body mass which could act to reduce the forces applied to the knee. The tightness of the seatbelt may also play a role in how much force is transferred to the meniscus because a loose seatbelt would allow for an increased travel distance of the torso. Further research may focus on determining which of these variables have the greatest effect on medial menisci injuries and what steps should be taken in order to reduce the risk of injury.

There are two possible situations that may apply a compressive load to the leg while twisting either the femur or tibia. In most cases, the occupant of the target vehicle has their right foot either on the brake pedal or on the floor of the vehicle so that their knee is significantly flexed at an angle between 30º and 90º. During the initial impact caused by the bullet vehicle, the foot may move backwards but then becomes planted on either the floor or brake pedal as the torso reverses directions and moves forwards relative to the vehicle. The forward movement of the hips causes the knees to move apart and the thighs to angle outwards since the legs pivot about the hips. At this point, the foot and hips can both be considered fixed joints with two links connecting them with a third joint at the knee. In order for the knee to move laterally, the thigh can either translate across the seat top or it can translate while also rotating about the hip joint. If there is pure translation of the thigh with no rotation, the forces will tend to bend the knee outwards, which creates compression and torque within the knee. If there is sufficient rotation about the hip joint as well as translation, these forces can be avoided and there will not be excessive forces applied to the meniscus. One reason that the thigh would primarily slide across the seat instead of rotating could be the amount of friction between the upper leg and the seat. The sudden impulse applied to the leg may also cause the leg to quickly translate without providing the time to properly rotate to avoid injury. The seat height and strength of the subject's legs can also factor in to the amount of knee movement in a rear end collision. The angle of the leg prior to impact would also influence the amount of torque placed on the knee and thus the degree of injury inflicted on the meniscus.

A second way to create compression while producing an axial torque could be from the position of the foot just prior to the rear end impact. If the driver of the target vehicle has their right heel resting on the foot pan floor in between the gas and brake pedal, and is seated properly, their leg is flexed approximately 72º. When the car is stopped at a traffic light, it is assumed that the ball of the right foot is on the brake pedal which means that the foot is angled towards the midline of the body. Since many brake pedals are located towards the middle of the seat, the leg is required to rotate internally so that the toes can reach the pedals while keeping the heel planted on the floor. This position naturally internally rotates the tibia while the femur remains in approximately the same position, straining the knee ligaments. During impact, the foot will plant itself on the brake pedal due to the friction between the foot and the pedal and this will create a compressive force on the knee. The increased muscle tension of the leg required to depress the brake pedal may also contribute to a higher level of compression within the meniscus. Any additional lateral movement of the knee would introduce more torque that may be sufficient to tear the meniscus.

A direct blow to the knee could be a possible way to tear the meniscus since it can move the tibia a significant distance in relation to the femur. A lateral impact force of sufficient magnitude to the knee from the outside could tear both the ACL and the medial meniscus. Such a force may be possible if the legs move laterally, swinging about the hips, and strike either the center console, steering column, or the vehicle door. Another possibility would be a direct impact to the front of the knee which would serve to disrupt the ligaments of the knee. This may happen if the occupant of the target vehicle is not wearing a seatbelt or if it is loose, allowing the entire body to rebound off the seat

cushion and travel far enough for the knee to hit the dashboard. An offset rear end impact where the bullet vehicle does not strike the target vehicle squarely in the back would direct the force in a side-to-side and/or front-to-back line of action. This would provide a lateral component of the motion of any bodies within the target vehicle and could allow the legs to swing to one side, contacting the vehicle interior or increasing the torque applied to the knee. Direct impact of the knee or surrounding bones could definitely damage the medial meniscus but many of the reported knee injuries in rear end collisions do not report knee contact with the interior of the vehicle.

Another way to injure the medial meniscus would be to apply a tensile load to the leg, which would stretch the ligaments of the knee and stress the meniscus. This may happen if the driver's foot becomes trapped between or under the pedals while the body is accelerated rearward in relation to the vehicle during the initial impact. The friction of rubber shoes on the foot pan of the car may also be sufficient to keep the foot planted while the torso, hips, and upper legs move rearwards, creating a tensile force within the knee. This force may be sufficient to tear the ligaments such as the MCL, ACL, and meniscal periphery attachment points. This is the most unlikely scenario to occur since it would be difficult for the foot to remain completely stationary to allow sufficient forces to be applied.

Every vehicular accident is different and there are many variables that may affect the injuries and outcome of the impact but there are certain scenarios that would be most likely to injure the knee. For this study, only axial compression coupled with torque about the knee was studied in further detail since it seems to be the most likely to cause injury in these cases. While it may technically be possible, it would be extremely

difficult to create tensile loading conditions within the leg during normal operation of a vehicle. A direct impact force to the knee is more likely to occur, but would also create more severe injuries such as bone fracture. The most interesting case of meniscus injury is when the subject does not hit their knee on anything but still sustains a meniscal tear that has been caused by the accident.

1.10 Other CAD Knee Models

There are a few complete models of the knee published in papers but they are not freely distributed for use in continuing research. It was decided that a finite element analysis of the medial meniscus would be an effective way to model forces and determine how the tissue reacts under loading, since it is inexpensive and does not require special testing procedures. The first step was to attempt to create a three-dimensional model of the medial meniscus that could be used as a very simple way to determine its reaction to forces. Once a general model was generated using published meniscus dimensions and MRI images, further research was conducted to determine if a complete model of the knee was available. After an initial search of publications, an open source model of the knee was found and this became the primary protocol for the project.

Several simple medial meniscus models were created especially for this study to help understand how the meniscus reacts under certain applied loads. A semi-circular medial meniscus was constructed using AutoCAD (Autodesk, Inc., San Rafael, CA) with the inner edges tapering to the bottom of the model and can be seen in Figure 7. Another model was constructed with the inner edges tapering to the bottom as well as having a triangular cross section throughout the medial meniscus. The outside boundaries of these

models were created to the specifications of average published dimensions but it was difficult to represent the exact geometries (Stone et al, 2007). A set of MRI images of the knee were obtained from the NIH virtual body website and the cross sectional images were used to construct a three-dimensional model of the lateral meniscus. The MRI data set was composed of many pictures of the knee sliced at 3 mm intervals which were loaded into AutoCAD. The outline of the meniscus was traced using the spline tool and then the layers were lofted to produce a three-dimensional model that could be used in finite element testing. The result can be seen in the Figure 7 and this supplies a more accurate model of an anatomical meniscus.

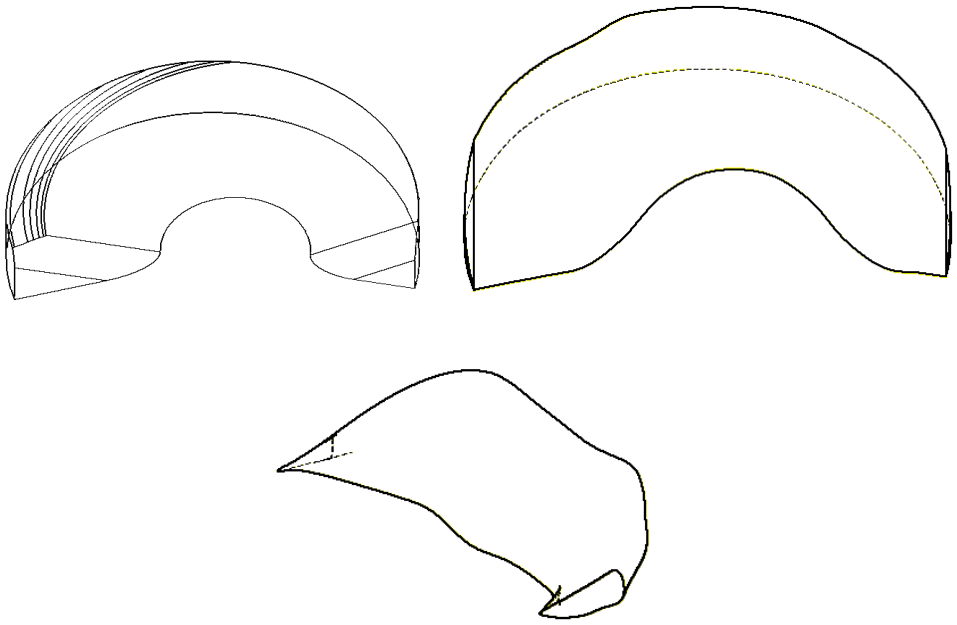

Figure 7- Medial Meniscual Models: (from top left to right) Cone shaped medial meniscus, wedge shaped medial meniscus, MRI based lateral meniscus

A femur model was needed to apply the loads to the meniscus in various configurations so two simple representations were created. One was a rigid body in the

shape of a ball with an attached shank, while the second was a cone shaped model that mated with the previous meniscal models. These femur models were added to the menisci to form a very simple model representing the loading of the meniscus bounded by a fixed bottom and a force applied on the top. The menisci material properties could then be described in finite element software, the boundary conditions set, and the femur modeled as a rigid body that transfers both a compressive and torsional load to the meniscus. It was decided to not use these models when a complete anatomical knee model became available, since it would provide a greater amount of accuracy while reducing the complexity of the current research.

1.11 Finite Element Analysis

Finite element analysis (FEA) is a way to solve a complex problem by breaking it into a certain number of individual problems. FEA is able to break a continuous structure into a finite number of equations that will approximate the behavior of the structure. This is done by assigning different elements and nodes throughout the area of interest to properly define the problem and allow boundary and loading conditions to be applied. Typically, a three-dimensional model is created in a computer automated design (CAD) program and then a meshing program is used to create a mesh throughout the model. This mesh is composed of equally spaced nodes that represent separate equations at each point, allowing a series of equations to be solved for the locally applied loads and material properties. A finer mesh is able to give a better approximation to the stresses and strains, but increases the complexity of the problem and requires a more powerful computer. Mesh optimization can be used to ensure that the mesh size is appropriate to

the problem and will maximize the quality of the results. Finite element analysis is iterative, meaning that the equations at each node are resolved for each time step of the simulation until the solution converges to a final answer. Finite element solvers can be either linear or non-linear, where linear solvers are used for small displacements, when the stresses are proportional to the strains and when the material is elastic. These conditions are not always met in real situations, so non-linear finite element solvers are used to model large displacements and are useful for complex problems, such as a knee joint, since it is more efficient than using other numerical techniques.

Finite element analysis provides a suitable alternative to cadaver or anatomical testing and has several benefits that allow for accurate research. Finite element analysis was chosen to be used in this study because it is more readily accessible, less expensive, and provides a level of accuracy that can be improved through research. Testing on cadavers requires special protocols and facilities that are not easily accessible to every researcher, while certain open source FEA programs can be used for free. Results of cadaver testing can be influenced by the preservation technique used and there may be previous unknown injuries that have pre-weakened the test site. Ex-vivo testing results can also be dependent on the techniques used and how the samples are handled during testing. Both of these testing methods are highly variable depending on the individual's anatomical structure and require a large sample to obtain accurate averages. In addition, many of these tests damage the tissue, often to failure, and the tissue is then useless for future testing. FEA allows for multiple trials to be performed without destroying a sample and can give an estimate for the forces seen internally. Finite element analysis is the appropriate first step to use when testing human biomechanics, since it is non-

invasive, inexpensive, and provides a way to test initial hypotheses quickly. Cadaver and ex-vivo testing are crucial elements in verifying the results of the FEA, but can be used after the initial analysis.

FEBio was chosen as the finite element solver for the analysis of the medial meniscus because it is a non-linear solver specifically designed for biomechanical applications. FEBio can run quasi-static simulations so that the effects of inertia are ignored or dynamic simulations which include inertia in the time dependent response of the system. A wide range of materials can be modeled to include rigid bodies, biphasic materials, or soft tissue using isotropic constitutive models. The materials used in the knee model were defined as either isotropic, meaning the material properties are identical throughout the part, or orthotropic, meaning that the material properties are identical at 90 degrees. Several boundary conditions can be applied to the model and include prescribed displacements, nodal forces, pressure forces, and frictionless contact between parts.

The basic equation for finite element analysis is given in Equation 1.1, where the partial derivative of the energy functional with respect to the grid point potential is zero.

$$\frac{\partial F}{\partial p} = 0 \tag{1.1}$$

Finite element analysis solves equations for each node found within the model to determine the displacements, strains, and stresses at each point. The first step was to divide the solution domain into discrete regions that are connected by nodal points. TrueGrid (XYZ Scientific, Livermore, CA) was used in the Open Knee model to generate high quality hexahedral meshes using surface projection methods. The equilibrium equations for each element used to find the deformational behavior and to determine the

strain through the relationship are described in Equation 1.2 (Finite Element Theory, 2006).

$$\{\Delta\varepsilon\} = [B]\left\{\frac{\Delta u}{\Delta v}\right\}_{nodal} \tag{1.2}$$

where matrix [B] represents the derivatives of the shape functions. The stresses can then be determined using Equation 1.3, where $\{\Delta\sigma\}$ is the stress vector and [D] is the constitutive matrix.

$$\{\Delta\sigma\} = [D]\{\Delta\varepsilon\} \tag{1.3}$$

The incremental potential energy (ΔE) can be found by subtracting the incremental work done by applied loads (ΔL) from the incremental strain energy (ΔW). The incremental work done by applied loads can be found using Equation 1.4.

$$\Delta L = \int_{vol}\{\Delta d\}^T\{\Delta F\}dVol + \int_{vol}\{\Delta d\}^T\{\Delta T\}dSurface \tag{1.4}$$

where $\{\Delta d\}^T$ are the displacements, $\{\Delta F\}^T$ are the body forces, and $\{\Delta T\}^T$ are the surface tractions.

At equilibrium, the potential energy is a minimum value and can be set equal to zero. The equilibrium equation for the total finite element model can be represented by Equation 1.5.

$$\delta\Delta E = \sum_{i=1}^{N}(\{\delta\Delta d\}_n^T)_i \begin{bmatrix} \int_{Vol}[B]^T[D][B]dVol\{\Delta d\}_n - \\ \int_{Vol}[N]^T\{\Delta F\}\,dVol - \int_{Surface}[N]^T\{\Delta T\}\,dSurface \end{bmatrix}$$

$$\delta\Delta E = 0 \tag{1.5}$$

$$\sum_{i=1}^{N}[K_E]_i(\{\Delta d\}_n)_i = \sum_{i=1}^{N}\{\Delta R_E\} \tag{1.6}$$

The element stiffness matrix is given in Equation 1.7.

$$[K_E] = \int_{Vol}[B]^T[D][B]\,dVol \tag{1.7}$$

The right hand side load vector is given in Equation 1.8.

$$\{\Delta R_E\} = \int_{Vol}[N]^T\{\Delta F\}\, dVol + \int_{Surface}[N]^T\{\Delta T\}\, dSurface \quad (1.8)$$

Once the global stiffness matrix has been created and the boundary conditions applied, the systems of equations can be solved to give the unknown nodal displacements (Finite Element Theory, 2006).

FEBio, the finite element solver, is able to automatically take the input loading and boundary conditions and solve the previous equations to find the stress and strain at each node. These values can then be compared to determine regions of increased stress and to see if the model will fail under certain conditions.

FEBio uses the full Newton's Method to solve the non-linear equations, which uses an implicit formulation to find the solution to the problem. The finite element solver looks to find the roots, or where the equation equals zero, of the governing equations since the solution is at the minimum point of the equation. This method finds the solution using a quadratic (i.e., involving a square root), asymptotic rate of convergence for the finite element problems and can be described by the general Equation 1.9. Since it is asymptotic and rapidly approaches the root, the solution can be solved quickly.

$$x_{n+1} = x_n - \frac{f(x_n)}{f'(x_n)} \quad (1.9)$$

A more detailed look at the Newton's Method shows that the stiffness matrix depends on displacement and requires an iterative approach for a successful solution, as can be seen in Equation 1.10.

$$\psi\left(u_{n+1}^{i+1}\right) \approx \psi\left(u_{n+1}^{i}\right) + \left(\frac{\partial \psi}{\partial u}\right)_{n+1}^{i} du_{n+1}^{i} = 0 \quad (1.10)$$

where u_{n+1} is the set of discretization parameters and u_n is the converged solution of the last step. The stiffness matrix is shown in Equation 1.11.

$$K_T = -\frac{\partial \psi}{\partial u} \tag{1.11}$$

which can be substituted into the previous equation to give Equation 1.12.

$$du_{n+1}^{i} = \left(K_T^i\right)^{-1} \psi_{n+1}^{i} \tag{1.12}$$

During each iteration, the stiffness matrix and the discretization parameter are updated, which can become computationally expensive and slow down the simulations time.

There are some problems with Newton's Method which include being difficult to calculate the derivative of the function and that the method may not converge to the root. This could result due to overshoot or a poor initial estimate of the root, but can be prevented by setting limits on the number of iterations used to find the solution. Second partial derivatives are needed for the calculation which may be difficult to actually find for some functions. Another downside is that it is required to store the Hessian matrix, which is also known as the stiffness matrix and is related to the material properties, and this requires a certain amount of memory that can slow down the computations. The positive aspects of using this method can outweigh the negatives since it is able to find the minima of the function very rapidly given the correct initial guesses and parameters.

The Quasi-Newton Method is an alternative to the full method that can be used to find the roots of the energy equations, but it requires an approximation to be made for the Hessian matrix. This method is easier to compute and, therefore, faster, since it allows for a greater rate of convergence. The governing equation used to describe the Quasi-Newton Method is shown in Equation 1.13.

$$x_{n+1} - x_n = A_{n+1}\left(\nabla f(x_{n+1}) - \nabla f(x_n)\right) \tag{1.13}$$

where x_n is the current point along the function, A_n is the Hessian, and f(x) is the energy function used to describe the system. While the current simulations used the Full

Newton's Method, future simulations could experiment with using the Quasi-Newton Method.

1.12 Stress and Strain

There are several stresses and strains found by FEBio and used in the comparison of results that will be discussed here to give a better understanding of their meaning. The Green-Lagrange strain tensor is defined in Equation 2.1 and is used for large deformations.

$$E = \frac{1}{2}(C - 1) \tag{2.1}$$

where

$$F = \frac{\partial \varphi}{\partial X} \quad \text{is the deformation gradient tensor} \tag{2.2}$$

$$C = F^T F \quad \text{is the right Cauchy-Green deformation tensor} \tag{2.3}$$

$$B = F F^T \quad \text{is the left Cauchy-Green deformation tensor} \tag{2.4}$$

The small strain tensor can be defined in Equation 2.5 and is used for small strains only while being dependent on the displacements at each point.

$$\varepsilon = \frac{1}{2}\left(\frac{\partial u}{\partial x} + \left(\frac{\partial u}{\partial x}\right)^T\right) \tag{2.5}$$

The Kirchoff stress tensor is found in Equation 2.6, with σ being the Cauchy stress, and expresses the stress relative to the reference configuration for finite deformations.

$$\tau = J\sigma \tag{2.6}$$

The Second Piola-Kirchoff stress is used to relate forces in the reference configuration to the area in the reference configuration and is defined in Equation 2.7.

$$S = 2\frac{\partial W}{\partial C} = \frac{\partial W}{\partial E} \tag{2.7}$$

where W is the strain energy function and C is the right Cauchy-Green deformation tensor. The Cauchy stress is used for small deformations and can be derived from the Second Piola-Kirchoff stress in isotropic hyperelasticity by using Equation 2.8.

$$\sigma = 2\{(\mathrm{W}_1 + \mathrm{I}_1\mathrm{W}_2 + \mathrm{I}_2\mathrm{W}_3)B - (\mathrm{W}_2 + \mathrm{I}_1\mathrm{W}_3)B^2\} + \mathrm{W}_3\mathrm{B}^3 \tag{2.8}$$

with

$$\Psi_1 = \frac{\partial \mathrm{W}}{\partial I_1} \qquad \Psi_2 = \frac{\partial \mathrm{W}}{\partial I_2} \qquad \Psi_3 = \frac{\partial \mathrm{W}}{\partial I_3} \tag{2.9}$$

Finally, the effective stress is defined as the uniaxial equivalent of a multi-axial stress state, and can be composed from the principle stresses as seen in Equation 2.10. The effective strain can be calculated in the same way but with using the principle strain values. The effective stress and strain will be the main variables used for comparison in the analysis of the simulation results.

$$\sigma_e = \sqrt{\frac{1}{2}\{(\sigma_1 - \sigma_2)^2 + (\sigma_1 - \sigma_3)^2 + (\sigma_2 - \sigma_3)^2\}} \tag{2.10}$$

These relationships form the basis for the analysis of the different types of stresses and strains presented in the results section.

1.13 Current Finite Element Model

A complete three-dimensional CAD model of the knee, called Open Knee (Erdemir, Sibole, 2010), was used in the simulation modeling and it included the femur, tibia, ligaments, menisci, and cartilages. Open Knee was created by the Musculoskeletal Research Laboratory at the University of Utah by gathering the geometries of the anatomical structures from MRI data sets, outlining each component, and importing them

into a 3D CAD modeling program. The data slices were then converted into three dimensional CAD models, meshed to be used in finite element analysis, and it was imported into PreView (MRL, 2010) to apply boundary and loading conditions. FEBio (MRL, 2010), a finite element solver, was used to run the simulation and compute the output variables and PostView (MRL, 2010) was used to visualize the results.

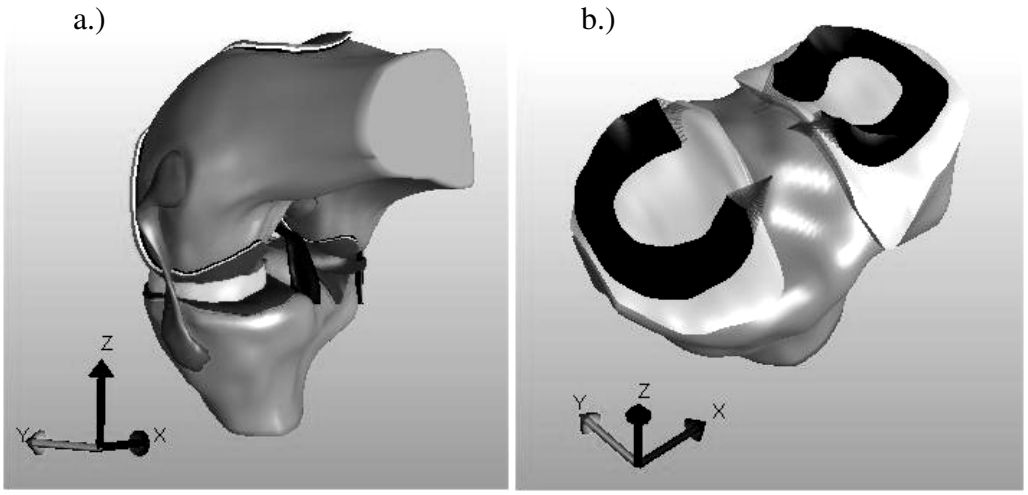

Figure 8: Open Knee Model of Right Knee (a.) and Meniscus with Femur Removed (b., posterior view)

This particular model, seen in Figure 8, was created from MRI images taken of the right knee of a five foot six, 170 lbs, 70 year-old female cadaver acquired from the National Disease Research Exchange. The knee specimen was imaged at the Biomechanics Laboratory of the Cleveland Clinic using a 1.0 Tesla extremity MRI scanner. Seventy MRI slices were made at 1.5 mm intervals of the knee in full extension in the saggital, coronal, and axial planes. The protocols used to image the knee followed the data published in Borotikar (2009). The files supplied on the Open Knee website include CAD models of each component of the knee in .iges format, a fully meshed

model of the knee in full extension using TrueGrid, Abaqus output files, and FEBio output files.

FEBio was used to complete various simulations with different loading conditions. This software was chosen over other programs, such as Abaqus, because it is an open source, non-linear finite element analysis package that was freely available. FEBio was designed to solve biomechanical problems, so it was a good match to test the reaction of the knee joint. In addition, previous analysis had been performed on a knee joint model using FEBio, allowing for only minor changes to complete the current testing. FEBio 1.3.0.1455 was used in the following simulations, with PreView 1.3.1.1332 and PostView 1.3.1.1272 being the pre- and post-processors, respectively.

Separate material properties were defined for each component used in the current finite element analysis to properly describe the knee joint and values for the material constants were taken from reported published literature. Table 2 shows the material properties used to define both the lateral and medial menisci.

Table 2: FEBio Model Parameters for Menisci

Parameter	**Value**
Density	1.5e-9 tonnes/mm^3
E_1	125 MPa
E_2	27.5 MPa
E_3	27.5 MPa
v_{12}	0.1
v_{23}	0.33
v_{31}	0.1
G_{12}	2 MPa
G_{23}	12.5 MPa
G_{31}	2 MPa
C	1
K	10 MPa

All contact between articulating surfaces of the knee joint were modeled as frictionless contact since actual joint friction within the knee is negligible. The femur and tibia were modeled as rigid bodies which allowed for rigid body kinematics and decreased the overall complexity of the simulation. The densities defined for these two bones can be found in Appendix B and the femur and tibia were mass scaled approximately 1000 times the value for dry cortical bone (Erdemir, Sibole, 2010). The overall mass and inertia of the bones are not accurate since they are modeled as shell elements in FEBio but this can be ignored for quasi-static or slow moving dynamic simulations.

The ligaments were defined to be nearly incompressible, transversely isotropic hyperelastic fiber material with the strain energy function shown in Equation 3.1. This type of material was assigned to the medial and lateral collateral ligaments and the anterior and cruciate ligaments.

$$W = C_1(I_1 - 3) + C_2(I_2 - 3) + \frac{K}{2}(\ln(J))^2 + F(\lambda) \tag{3.1}$$

with

$$\lambda\frac{\partial F}{\partial \lambda} = \begin{matrix} 0 & \lambda < 1 \\ C_3(e^{C_4(\lambda-1)} - 1) & 1 \le \lambda < \lambda_m \\ C_5 + C_6\lambda & \lambda \ge \lambda_m \end{matrix} \tag{3.2}$$

$$I_1 = trC \tag{3.3}$$

$$I_2 = \frac{1}{2}[(trC)^2 - trC^2] \tag{3.4}$$

$$I_3 = detC = J^2 \tag{3.5}$$

where,

C_1 and C_2 are Mooney-Rivlin constants (MPa), C_3 to C_6 are fiber material constants, K is the bulk modulus, I_1 is the first invariant of the deviatoric right Cauchy-

Green deformation tensor, I_2 is the second invariant of the deviatoric right Cauchy-Green deformation tensor, J is the determinant of the deformation gradient tensor, F is the strain energy density component, λ is the deviatoric part of the stretch along fiber direction, and λ_m is the straightened fiber stretch. The values of the material properties used to evaluate these equations in FEBio can be found in Appendix B. It should be noted that the constant C_2 was set to zero in the simulations, effectively reducing the ground substance of the ligaments to a Neo-Hookean material.

The tibial and femoral cartilage was described as nearly incompressible Mooney-Rivlin material, which is a hyperelastic material with a special strain energy function given in Equation 3.6. The strain energy function for the cartilage within the finite element model used the same parameters as described previously, but is given in a slightly different form and used the values used in Appendix B.

$$W = C_1(I_1 - 3) + C_2(I_2 - 3) + \frac{K}{2}(\ln(J))^2 \tag{3.6}$$

Both the medial and lateral menisci were defined as Fung orthotropic hyperelastic material with the strain energy function given by Equations 3.7 to 3.10.

$$W = \frac{1}{2}c(e^Q - 1) \tag{3.7}$$

$$Q = c^{-1}\sum_{a=1}^{3}[2\mu_a A_a^0 : E^2 + \sum_{b=1}^{3}\lambda_{ab}(A_b^0 : E)] \tag{3.8}$$

$$\begin{bmatrix} \lambda_{11}+2\mu_1 & \lambda_{12} & \lambda_{13} \\ \lambda_{12} & \lambda_{22}+2\mu_2 & \lambda_{23} \\ \lambda_{13} & \lambda_{23} & \lambda_{33}+2\mu_3 \end{bmatrix} = \begin{bmatrix} \frac{1}{E_1} & \frac{-v_{12}}{E_1} & \frac{-v_{31}}{E_3} \\ \frac{-v_{12}}{E_1} & \frac{1}{E_2} & \frac{-v_{23}}{E_2} \\ \frac{-v_{31}}{E_3} & \frac{-v_{23}}{E_2} & \frac{1}{E_3} \end{bmatrix} \tag{3.9}$$

$$\begin{aligned} \mu_1 &= G_{12} + G_{31} - G_{23} \\ \mu_2 &= G_{12} - G_{31} + G_{23} \\ \mu_3 &= -G_{12} + G_{31} + G_{23} \end{aligned} \tag{3.10}$$

where A^0 relates to the initial direction of material axis, E is the Green-Lagrange strain tensor, λ is Lame's first parameter, μ is Lame's second parameter, E is the Young's modulus (MPa), G is the shear modulus (MPa), v is Poisson's ratio, and K is the bulk modulus.

The parameter values used in the simulations (Table 2) were compiled from published literature and were used previously in the original Open Knee models. The Young's modulus, Poisson's ratio, and shear modulus each vary with the principle axes which provide a better approximation to the strength of the meniscus with respect to the radial and circumferential directions.

The meniscal horn attachments were modeled as linear springs that attached each node on the meniscal horn to a node on the tibia. The spring stiffness (k_i) was found by using Equation 3.11, where E is the Young's modulus of the meniscal horn, A is the total horn face area, L is the spring length, and N is the number of nodes.

$$k_i = \frac{E}{NL_i}A \tag{3.11}$$

The Open Knee model had model coordinates assigned to it, which can be seen in Figure 8, and is consistent throughout the stress and strain distribution maps discussed later. The x-axis was defined as the flexion axis of the knee, the y-axis was defined as the posterior-anterior axis, and the z-axis was defined as the superior-inferior axis (Erdemir, Sibole, 2010). The origin of the axis was defined to be at the center of the joint and in between the medial and lateral condyles of the femur.

2. Methods and Materials

The Open Knee files were modified to accommodate different flexion angles and applied forces that may be observed during rear end collisions. National Highway Traffic Safety Administration data shows that the average knee flexion angle while sitting in the driver's seat is approximately 72º (NHTSA,2011). The simulations presented here were performed with the knee model flexed at various degrees to determine the medial meniscal reaction to compressive loads and axial torque. The simulations were run using the dynamic setting because initial testing of the Open Knee model proved that the kinematics and stresses and strains were identical to a simulation using the quasi-static setting. It was found that using this dynamic setting reduced the computation time by more than half and was much more efficient computationally. Even though the setting used was dynamic, the slow moving simulation allowed inertial effects to be ignored, effectively performing a quasi-static simulation of the model. Each simulation was performed using a 64-bit dual core PC laptop computer with 4 GB of RAM. The computational duration of the simulations varied with the complexity of the applied boundary conditions and loads, but ranged from five to over fifty hours to complete. This study progressed from low applied loads to higher values to provide a starting point for comparison and to decrease the complexity of the simulations.

2.1 Model Validation

Some points of comparison were used to help give an idea on the accuracy and validity of the present model. A previous study that applied 1000 N compressive loading to the neutral knee found that the medial tibial cartilage had a maximum compressive

stress of 2.5 MPa while the lateral side had a maximum of 2.7 MPa (Bendjaballah et al., 1995). In the current finite element model loaded under the same conditions, it was found that the maximum compressive stress was 1.6 MPa on the medial side and 3.14 MPa on the lateral side, as can be seen in Figure 9. This shows the trend that the lateral side bears the larger compressive stress but there is a good deal of variation between these two studies. In another study, a varus torque of 15 Nm was found to produce a stress of 1.4 MPa in a similar type of model (Bendjaballah et al., 1997). In the current model, the maximum stress was found to be only 0.611 MPa when the applied torque was 20 Nm. This suggests that further validation for both models is needed in order to give a better understanding of which values are accurate.

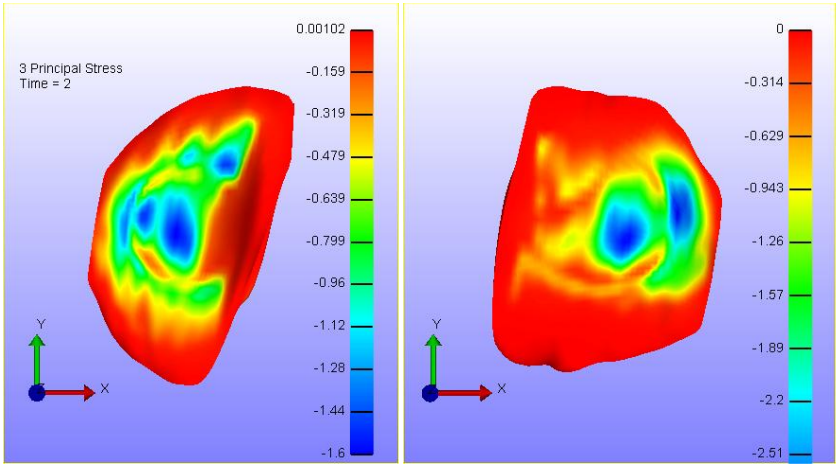

Figure 9: Compressive Stress in Medial (left) and Lateral (right) Tibial Cartilage under 1000 N Compressive Loading

Several test trials were run with varying parameters to determine their effects on the model (Tichon, Peterson, 2011). In the original simulation, at 400 N compressive load was applied to the neutral knee using the original bone density of 1.132e-6 tonnes/mm^3 and the stress was found to be 4.503 MPa. When the same simulation was run again but with the density changed to 1.5e-6 tonnes/mm^3, the stress increased to 5.585 MPa. This shows that even though the simulations were run quasi-statically there

is some variation in the results with changes in density values. This is an important factor to investigate in future work in order to determine a density value that best represents the femur and tibia. A second trial was run that applied a 100 N tensile load to the knee while it was in the neutral position to determine the reaction within the medial meniscus. The maximum effective stress was found to be 9.08e-13 MPa, while the effective strain was found to be 2.44e-14. These values are extremely small (i.e., essentially zero), which is to be expected since there was no loading on the menisci due to the fact that the periphery was not attached to the femur. A more complete model of the knee would include the medial meniscus attached indirectly to the femur through the medial collateral ligament with a tensile force through the femur at the attachment site. Future testing may include a more extensive analysis of the effects of changing different variables on the stresses and strains found within the medial meniscus.

2.2 Simulations

For this paper, several types of applied loading conditions were imposed on the knee model to determine the reaction within the medial meniscus. The first type of loading studied was pure compression of the knee joint by applying a force through the femur in the direction of the long axis of the tibia, or the z-direction, while keeping the tibia fixed and with the knee in the neutral position. Another loading condition studied was external axial torque about the long axis of the tibia that served to rotate the femur externally with the tibia remaining fixed. Knee flexion was also studied by prescribing an amount of rotational displacement on the femur about the x-axis of the model so that the tibia remained fixed but the femur underwent passive flexion. While compression,

axial torque, and flexion were the main variables examined in the simulations, one simulation was included to compare the effect of varus torque imposed on the knee. This varus torque was imposed about the y-axis of the model with the tibia remaining fixed and the femur rotating medially, effectively pinching the medial meniscus. Figure 10 illustrates the directions for the various loading conditions used in the simulations described.

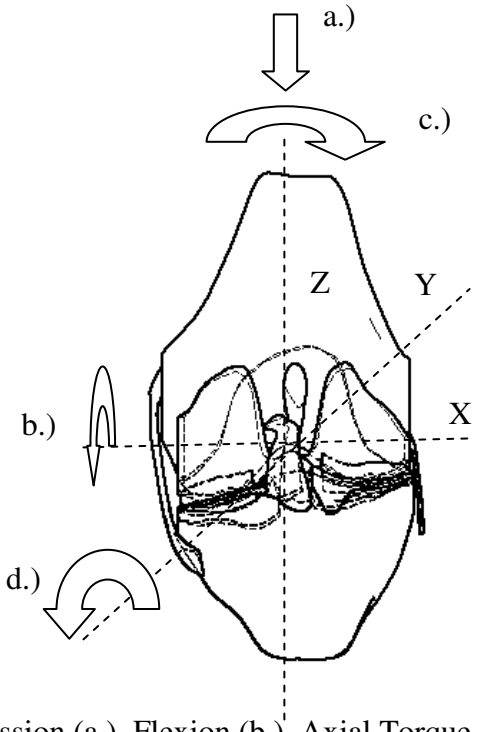

Figure 10: Compression (a.), Flexion (b.), Axial Torque (c.), and Varus Torque (d.) on the Knee (Posterior View)

To date, twenty-seven simulations have been run using a combination of different loading conditions and magnitudes of forces, as seen in Table 3. The first eleven simulations kept the knee in the neutral position but applied increasing compressive loads that reached 1333 N. Simulations 12 to 15 kept the compressive loading constant but increased the axial torque from 16 to 40 Nm. Simulation 16 was the original Open Knee

model test simulation while Simulation 17 to 20 increased the compressive loading with the knee flexed to 72 degrees. Simulations 21 to 25 combined all of the variables by increasing the compression and axial torque applied to the knee when it was flexed at 72 degrees. The last two simulations were meant to be a quick comparison of the effects of varus torque on the knee in the neutral position and under low compressive loading.

Table 3: Summary of Simulations and Applied Forces (*Varus Torque)

Simulation	Compression (N)	Flexion (deg)	Torque (Nm)
1-11	100-1333	0	0
12-15	200	0	16-40
16	100	45	0
17-20	100-500	72	0
21-25	200-300	72	4.8-10.4
26-27	200	0	10-20*

3. Results

The maximum stresses and strains within the medial meniscus were determined for each simulation since these values would indicate if an injury would occur, and their corresponding distribution maps were studied to determine the location of these maximum values. The maximum effective Cauchy stresses and Green-Lagrange strains, third principle stresses and strains, and shear stresses and strains found within the medial meniscus are presented in Table 4. The values indicate the largest stresses and strains found among all of the nodes comprising the medial meniscus, independent of orientation. The effective stresses and strains represent the largest tensile values seen within the meniscus and are generally greater in magnitude than the other variables. The third principle values represent the compressive stresses and strains within the sample,

which is important since the meniscus is likely to fail in either tension, compression, or by shearing. While all three types of stresses and strains are important in determining the failure mode of the model, the primary variable studied will be the effective stress since it represents the maximum tensile force per unit area that the medial meniscus sustains. Previous research had shown that the meniscus is more likely to fail in tension than through compressive or shear stress, so this will be the focus of this study. In the future, this study can be expanded to determine other failure modes due to shear stress that causes longitudinal or horizontal tears.

Table 4: Maximum Stresses and Strains in Medial Meniscus
(*Applied Varus Torque)

Applied Forces			***Output Variables***					
Compression (N)	**Flexion (deg)**	**Torque (Nm)**	**Eff. Stress (MPa)**	**Eff. Strain**	**3rd Stress (MPa)**	**3rd Strain**	**Shear Stress (MPa)**	**Shear Strain**
100	0	0	1.191	0.061	0.602	0.028	0.566	0.033
200	0	0	1.936	0.093	1.049	0.043	0.934	0.052
300	0	0	2.483	0.113	1.397	0.050	1.265	0.065
400	0	0	2.894	0.126	1.566	0.060	1.545	0.072
500	0	0	3.358	0.140	1.885	0.072	1.848	0.080
600	0	0	3.902	0.149	2.138	0.077	2.130	0.086
700	0	0	4.307	0.158	2.332	0.080	2.379	0.091
800	0	0	4.818	0.167	2.504	0.090	2.659	0.096
900	0	0	5.353	0.186	2.646	0.101	2.929	0.103
1000	0	0	5.859	0.195	3.017	0.103	3.185	0.109
1333	0	0	7.382	0.219	3.870	0.110	3.968	0.123
200	0	16	2.411	0.106	1.049	0.043	1.305	0.061
200	0	24	2.603	0.114	0.944	0.048	1.394	0.065
200	0	30	2.292	0.102	0.956	0.045	1.251	0.058
200	0	40	2.299	0.102	0.939	0.046	1.261	0.058
100	45	0	1.614	0.076	1.101	0.052	0.905	0.041
100	72	0	1.102	0.055	1.129	0.047	0.728	0.032
150	72	0	1.179	0.059	1.144	0.052	0.730	0.034
300	72	0	2.099	0.100	2.403	0.074	1.313	0.052
500	72	0	5.759	0.289	3.322	0.116	2.298	0.151
209	72	4.8	1.554	0.062	1.437	0.057	0.892	0.033
255	72	8	1.947	0.098	2.036	0.076	1.089	0.056
296	72	6.2	2.055	0.094	2.183	0.086	1.093	0.054
302	72	8.7	2.183	0.110	2.437	0.099	1.245	0.063
308	72	10.4	2.372	0.115	2.577	0.083	1.521	0.052
200	0	10*	2.408	0.107	1.085	0.049	1.298	0.061
200	0	20*	2.461	0.109	1.103	0.053	1.337	0.062

A comparison of the maximum effective stresses and strains within the medial meniscus revealed several trends that have been summarized in the graph and table included below. Figure 11 shows the increasing relationship between applied compressive loading of the knee and the stress for the knee while in the neutral and flexed positions. With the knee in the neutral position, there is an almost perfect linear increase in the stress but the effective stress had the greatest magnitude. The compressive and shear stress both had very similar curves due to the fact that the values for each stress had little variation while the effective stress was not only greater in magnitude, but had a steeper slope to the curve. Less data points were determined for the knee flexed at 72º due to a limited amount of simulations performed. The maximum effective stress of the meniscus with the knee flexed was seen to follow an exponential type curve where the first points did not show much increase but then drastically increased. It was seen that when the compressive force applied to the knee in the flexed position reached 37% of the largest load applied to the neutral knee, the effective stress had reached a level of 78% of the largest stress seen when the knee was in the neutral position. The maximum compressive stress found within the medial meniscus followed an opposite increasing trend by increasing more rapidly at low loads and then flattening off. The maximum shear stress followed an increasing linear trend with the magnitude less than the other two types of stresses.

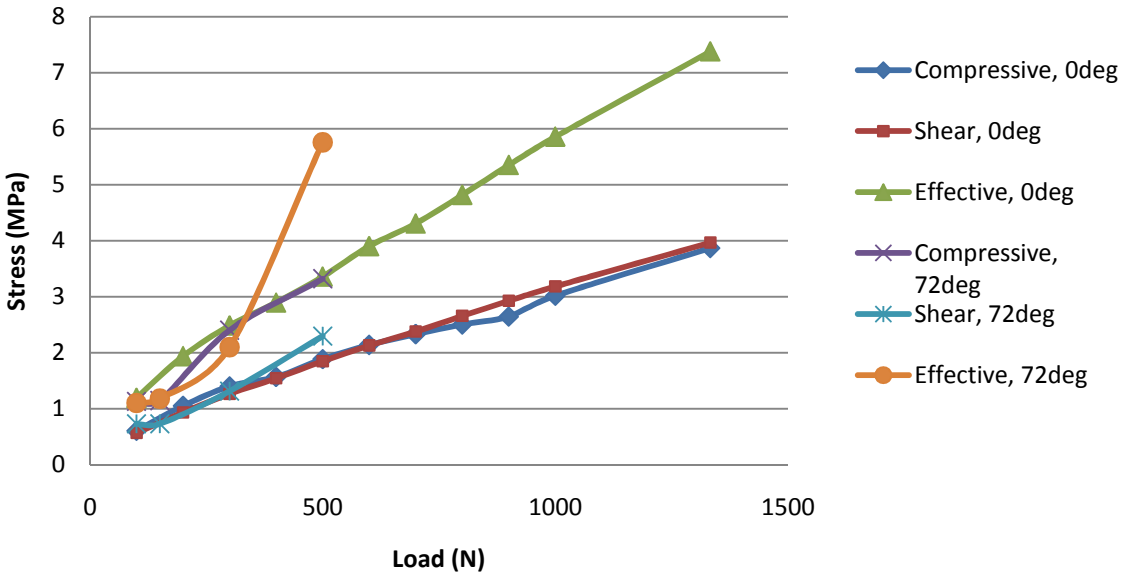

Figure 11: Maximum Stresses in Medial Meniscus

It was found that a very large increase in compression on the knee in the neutral position without additional torque increased the effective stress and strain, but the increase did not directly correlate to the applied loading since the increase of the stress and strain remained well below the increase of the compression. It was seen that a 50% increase in axial torque applied to the neutral knee only increased the stress and strain by 8% for relatively low torques. When the torque was increased to levels over 24 Nm the stress and strain actually decreased by 12%, showing that large axial torque does not effectively increase the stress or strain within the meniscus. An increase in the knee flexion angle from 45 degrees to 72 degrees served to significantly decrease the effective stress and strain while under a low compressive load, as can be seen in Table 5. When increasing compressive loads were applied to the knee flexed at 72 degrees, the stress and strain increased by slightly more than the same percent, which is significantly more than when the knee was in a neutral posture. The combination of increased compression and axial torque applied to the knee flexed at 72 degrees increased the effective stress and

strain by 153% and 185%, respectively. Notably, a 200% increase in varus torque while under a low compressive load had almost no effect on the stress and strain since they only increased by 2% each.

Table 5: Percent Change in Applied Forces and Resulting Stress and Strain

Compression	Torque	Flexion	Effective Stress	Effective Strain	Comments
1333%	0%	0%	620%	359%	Neutral knee
0%	150%	0%	108%	108%	Low torque
0%	166%	0%	88%	89%	High torque
0%	0%	160%	68%	72%	Low compression
500%	0%	0%	523%	525%	For flexed knee
147%	217%	0%	153%	185%	For flexed knee
0%	200%	0%	102%	102%	Varus torque

The regions of maximum stress and strain were relatively consistent throughout the simulations and occurred primarily in the posterior horn, the mid-body, and along the inner edge of the medial meniscus. The effective stress distribution maps of select trials shown in Figure 12 through 17 supports the observation that many reported meniscal injuries include tears to the posterior horn and propagate from the inner to the outer edge of the meniscus. In general, the regions of high stress and strain are shown as the red and orange regions, located primarily along the edges, and low stress and strain are shown as the dark blue areas, found in the anterior and middle regions.

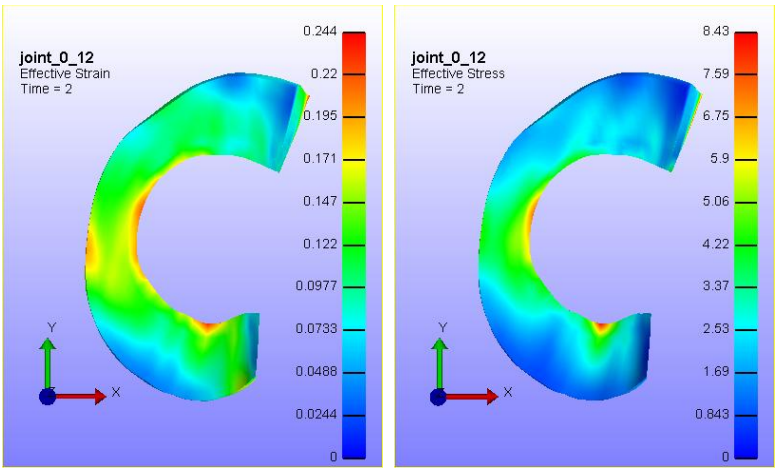

Figure 12: Superior View of Medial Meniscus: Maximum Effective Stress and Strain 1333 N, 0º Flexion, 0 Nm Torque

Figure 12 shows that the regions of maximum effective stress and strain occurred primarily along the inner edge of the mid-body and posterior horn of the medial meniscus when a pure compressive force was applied to the femur. The maximum stress value seen throughout the meniscus was found to be 7.382 MPa while the maximum strain was 0.219. When a low compressive force coupled with an axial torque was applied to the neutral knee, the maximum stress was 2.603 MPa, the maximum strain was 0.114, and these values occurred along the inner edge of the mid-body and posterior horn, as can be seen in Figure 13.

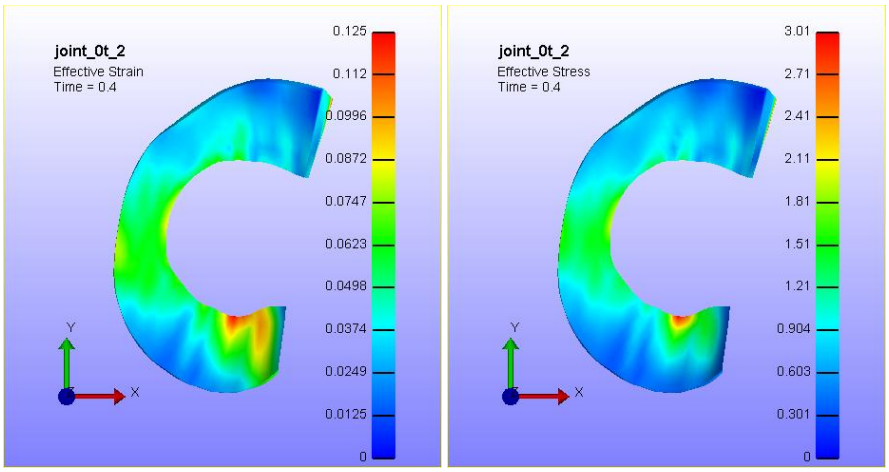

Figure 13: Superior View of Medial Meniscus: Maximum Effective Stress and Strain
200 N, 0º Flexion, 24 Nm Torque

Figure 14 shows that as the knee is flexed to 45 degrees, there are regions of increased stress and strain not only in the mid-body and posterior horn, but also the anterior horn of the meniscus. The maximum effective stress was 1.614 MPa and the strain was 0.076 for this simulation.

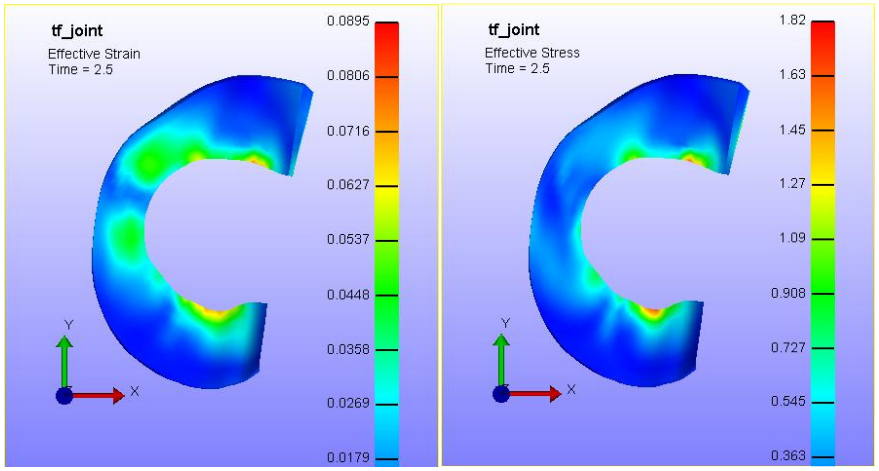

Figure 14: Superior View of Medial Meniscus: Maximum Effective Stress and Strain
100 N, 45º Flexion, 0 Nm Torque

When the compressive force was increased to 500 N and the flexion angle increased to 72 degrees, the maximum stress was 5.759 MPa and the maximum strain was 0.289. In this simulation, there was some increased stress and strain throughout the

mid-body, but the primary region was in the anterior horn and there was a large amount of deformation, as seen in Figure 15. This deformation is the result of the meniscus not being attached at its periphery to the tibia but shows there could be potential for forces to tear the meniscus.

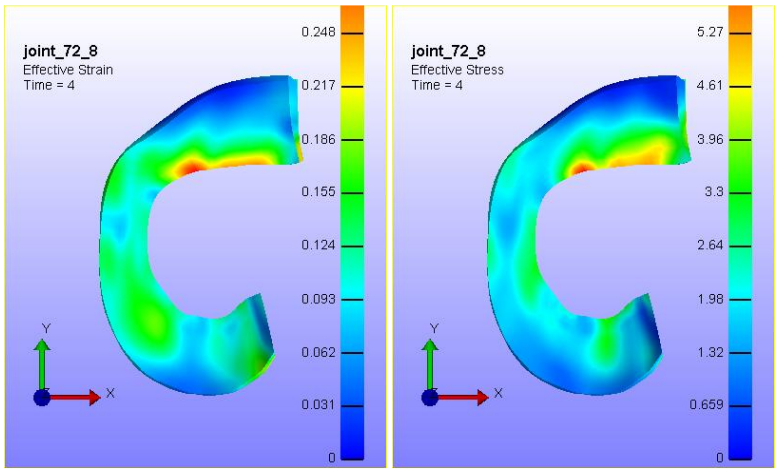

Figure 15: Superior View of Medial Meniscus: Maximum Effective Stress and Strain 500 N, 72º Flexion, 0 Nm Torque

When 308 N of compressive force was coupled with 10.4 Nm axial torque and flexion, the maximum stress was 2.372 MPa and the maximum strain was 0.115. These values were found along the inner edge of the anterior and posterior horns and can be seen in Figure 16.

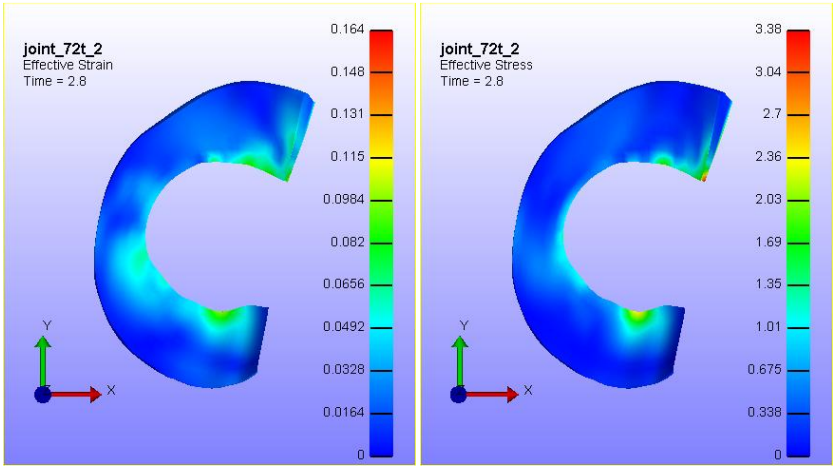

Figure 16: Superior View of Medial Meniscus: Maximum Effective Stress and Strain 308 N, 72º Flexion, 10.4 Nm Torque

Applying a varus torque of 10 Nm increased the maximum stress to 2.461 MPa and the maximum strain to 0.109, found along the inner edge of the mid-body and posterior horn, as can be seen in Figure 17.

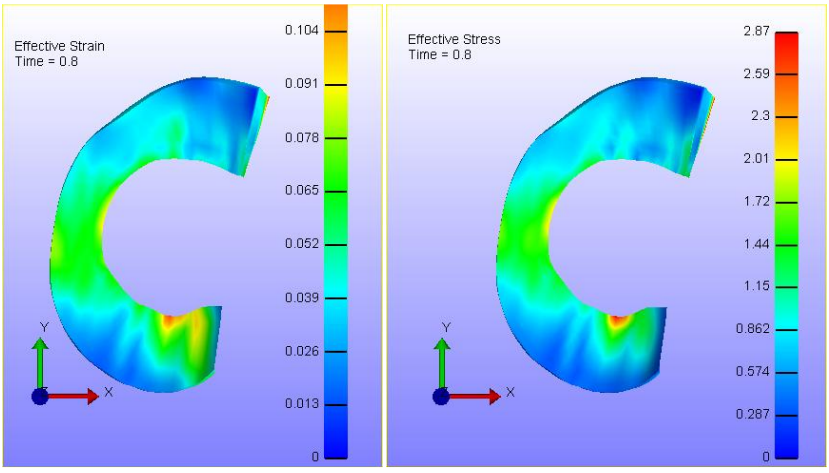

Figure 17: Superior View of Medial Meniscus: Maximum Effective Stress and Strain 200 N, 0º Flexion, 10 Nm Varus Torque

4. Discussion

The finite element simulations of the knee loaded under various conditions proved to give several interesting results that will help to better understand injury of the medial meniscus. In the simulations presented here, stress and strain increased as the compressive load imposed by the femur on the cartilages and menisci of the knee was increased. Increasing axial torque also served to increase the effective strain in some cases, but may not have a large effect after a certain magnitude of torque. Flexion of the knee decreased the stress and strain within the medial meniscus in some cases but the amount of change was influenced by other applied loading conditions. The combination

of these results can describe the medial meniscal reaction to forces that could be found in a low-speed rear end collision.

When the compressive load in the direction of the long axis of the tibia remained at 100 N and the flexion angle was varied between simulations, there was variation within the resultant effective stress seen within the medial meniscus. When the knee was flexed to 45 degrees, the stress increased by 136% as compared to the knee in the neutral position but flexion to 72 degrees decreased the stress by 8%, as seen in Figure 18. The small variation in stress between 72 degrees and 0 degree of flexion under low compressive loads means that there is not a large effect on stress at high and low flexion angles. Further testing could be performed to determine if changing the flexion angle more extensively will produce a definitive peak in the medial meniscal stress, but it appears to be around 45 degrees from these results. When the compressive load was increased to 500 N, increased flexion did not have the same effect as lower loads. When the knee flexion angle was increased from 0 degrees to 72 degrees, the effective stress increased by 72%, which is much different than the 15% reduction in stress seen while under a 300 N compressive load. This could prove that as the compressive load increases, having the knee flexed will significantly increase the stress, and thus the likelihood of meniscal injury.

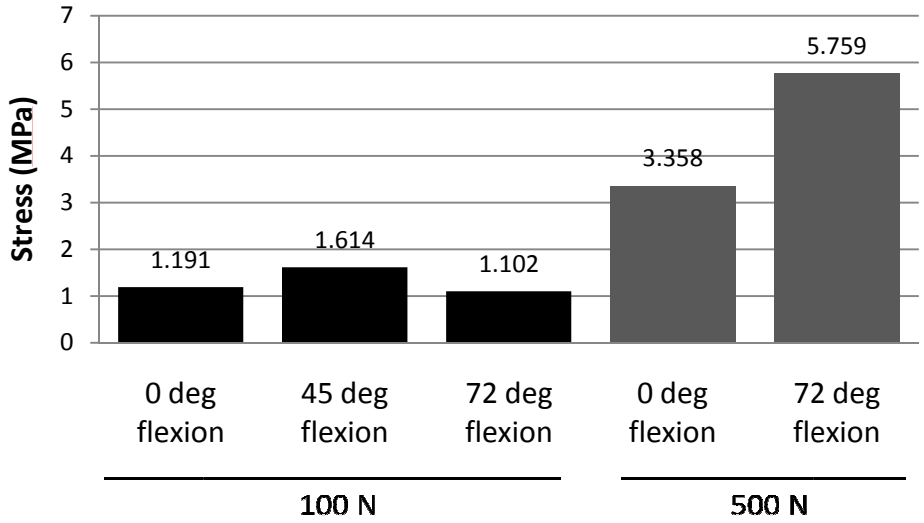

Figure 18: Maximum Effective Stress in Medial Meniscus, 100 N and 500 N Compressive Loading

A larger amount of simulations were performed under a compressive load of 200 N, allowing for comparison of the effect of several variables which is seen in Figure 19. As compared to the results of pure compression of the knee in the neutral position, an increased axial torque to 16 and 24 Nm each increased the stress, with 24 Nm torque increasing the stress 35% over the knee in the neutral position. When the torque was increased to higher levels, such as 30 and 40 Nm, the stress dropped to less than was seen with 16 Nm but remained greater than pure compression. The increase from 30 to 40 Nm did not produce a significant change in the effective stress found within the medial meniscus. This is primarily due to the structure and function of the femur and the stress concentration points changing as the larger axial torques moves the femur to a greater degree. Since the condyles of the femur are not perfectly spherical, it would be expected that there are bony protrusions that would appear at certain angles of the femur rotation and would serve to increase the applied forces in those corresponding areas. Varus torque applied with a compressive load of 200 N was also seen to increase the stress, presumably by increasing the compressive load since the meniscus is pinched by the

rotation of the femur. A 10 Nm varus torque increased the stress to almost the same level as when a 16 Nm axial torque was applied to the knee, or approximately 25% above the stress found in the meniscus when the knee was in the neutral position. An increase in the varus torque to 20 Nm increased the stress slightly but the change was small and remained less than the stress seen with 24 Nm of axial torque. These results suggest that even moderate torques can significantly increase the stress concentrations within the medial meniscus, possibly enough to sustain injury.

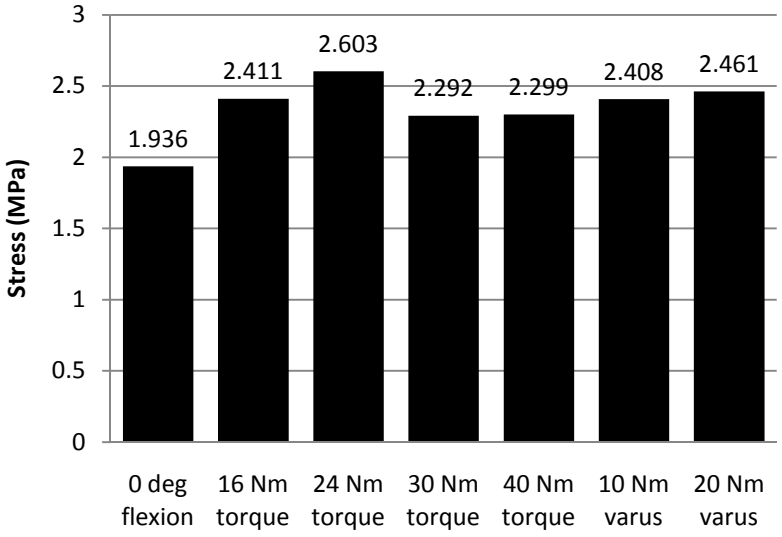

Figure 19: Maximum Effective Stress in Medial Meniscus, 200 N Compressive Loading

Figure 20 shows similar trends as observed previously but with larger magnitudes for the differences between trials. Under a 300 N load, increasing the knee flexion to 72 degrees reduced the corresponding effective stress by 15%, which is nearly double the change seen with a 100 N compressive load. The combination of flexion and low axial torque produced stresses less than when the knee was in the neutral position but higher than just flexion and compression. The stress increased as the torque increased, as seen under 200 N, and may reach a maximum around 24 Nm of axial torque.

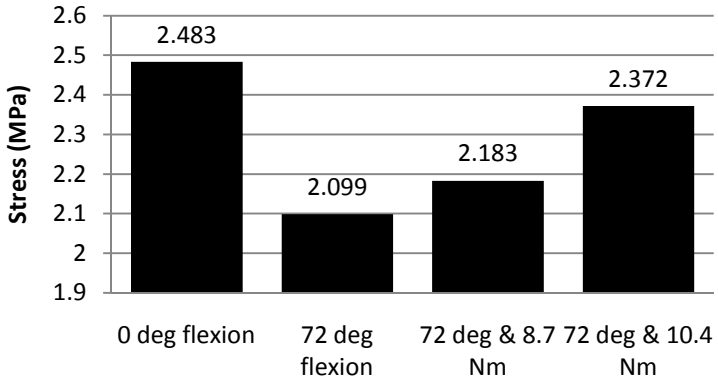

Figure 20: Maximum Effective Stress in Medial Meniscus, 300 N Compressive Loading

According to published research, the medial meniscal strength varies greatly with the region of the meniscus since the fiber orientation changes between layers and the anterior-posterior regions (Bullough et al., 1970). One paper showed that, on average, male medial menisci can have a maximum stress ranging from as little as 0.503 MPa to 9.307 MPa, depending on the orientation of the fibers (Bullough et al., 1970). Another paper reported average maximum stresses ranging from 2.66 MPa to 16.21 MPa in the radial and circumferential directions, respectively (Tissakht, Ahmed, 1995). The average values from these two papers are 4.905 and 9.44 MPa, showing that there is large variation in strength not only between the regions in the meniscus, but between tensile studies. This variation is important to note because it shows that a force sufficient to tear the meniscus of one subject may not produce injury in another due to individual characteristics and predisposed conditions of the subjects.

Using the average published strengths of the meniscus, several of the loading conditions produce stress that is above or close to the level that may produce injury. For example, compressive loading above 900 N on a knee in the neutral position produced stress greater than 4.905 MPa while flexion to 72 degrees and a 500 N compressive load

also produced stresses larger than this value. Since forces seen during normal gait can reach 1150 N, it is unlikely that these forces should cause injury because they remain within normal ranges for applied loads seen to the knee. If 9.44 MPa is used as the benchmark for injury, none of the current simulations were able to produce stress values great enough to cause injury. Future research may be aimed at improving the finite element model to incorporate larger magnitudes of forces to determine the exact loading conditions required for injury.

Since the results followed several trends, the loading conditions necessary for medial meniscal injury can be extrapolated using the trends shown in Figure 21. Since the relationship between increasing compressive load and stress was found to be almost perfectly linear with a slope of 0.0049 MPa/N, it was found that a compressive load of 1744 N would produce a stress of 9.44 MPa. This shows that if the knee is in the fully extended position, it is likely that the medial meniscus will be injured at values greater than 1750 N, with higher values increasing the likelihood. A polynomial trend line was fitted to the data for increasing compression with the knee flexed to 72 degrees and used to find the force required for injury. Using the data found in these simulations, a 667 N compressive load while the knee is flexed to 72 degrees may produce a stress of 9.44 MPa and create a tear. Introducing an axial torque of up to 24 Nm or a varus torque would also help to increase the stress found within the meniscus and decrease the compressive load required to produce the same level of stress.

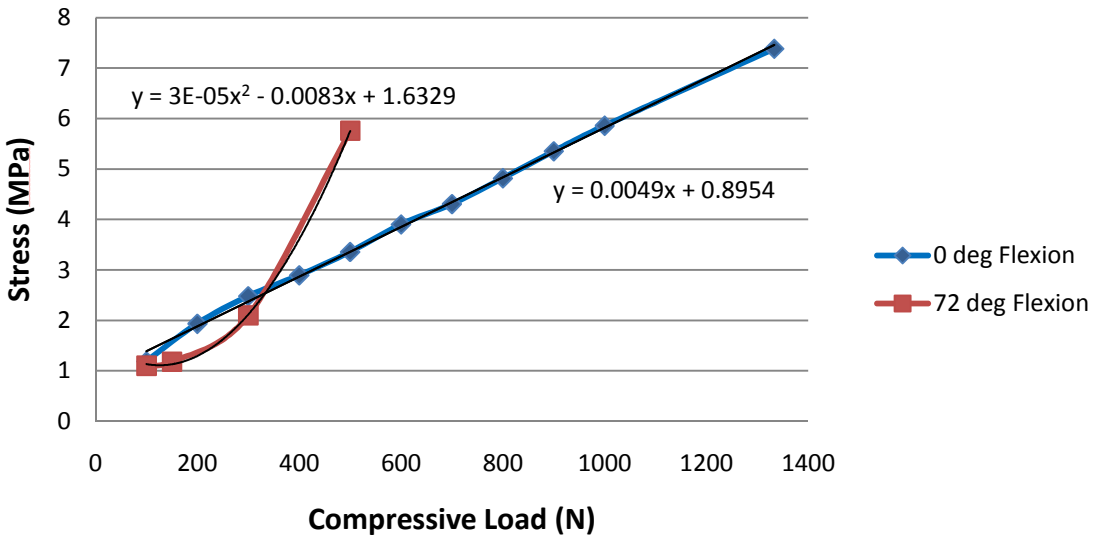

Figure 21: Extrapolation Curves for Effective Stress vs. Load

Previous studies have found that there are several differences in size and strength of the meniscus between genders and age groups. It was found that that tensile strength increases with age, a phenomenon that may be due to increased cross linking that reinforces the meniscus (Seedhom et al., 1972). It should be noted that a healthy aged meniscus may prove to be stronger, but the older the person is, the more chance of mechanical injury to the meniscus from activities. Since the menisci are avascular, they do not heal very well and any injury, even many years previous, will remain and create a stress concentration point that may make a future tear more likely. It was also found that females have stronger menisci than males and that, on average, they have smaller dimensions for all parts of their knee, including the medial meniscus (Yoshioka et al., 1987). In addition, people with a Body Mass Index (BMI) number less than 25 have smaller dimensions for all parts of the knee than people with a BMI over 25 (Hauch et al., 2009). This means that an obese man will likely have a larger meniscus than other subjects, meaning there is a greater surface area and potential for injury.

The stress and strain distribution maps also show several trends that provide insight into how the meniscus is injured. When the knee is loaded through compression and torque but remains in the neutral position, there is increased stress and strain in the mid-body and posterior horn of the meniscus. The largest values are found along the inner edge and there is a small region in the posterior horn that was consistent throughout the simulations but grew with increasing magnitude of compressive loading. When the knee was flexed, there was a region in the anterior horn that also had increased stress and strain and occurred along the inner edge. This is consistent with reports that medial meniscal injuries often occur in the posterior horn but that injuries can be sustained in other regions as well. The most common type of meniscal tears are oblique and transverse tears, which both start from the inner edge and spread outward, and this is perfectly shown in the stress and strain distribution maps (Erskine, 1950).

These simulations show that is it possible for the medial meniscus to be injured with the right combination of applied forces and if the meniscus is naturally weaker at some points. Injury could occur since the inner edge of the meniscus is naturally thinner than the outer edge and the increased stress concentrations in that area would make it easy for a tear to propagate from the inner to outer edge. Variation between individuals in the orientation of fibers within the meniscus could provide a point of weakness that would allow a tear to begin with relatively low applied force.

4.1 Study Limitations

There are several limiting factors that are incorporated into this study and include that there is limited research on the subject of torn menisci during various activities. There is

no published information on injury of the medial meniscus in relation to a rear end collision, making it difficult to find any concrete data to compare the previous results to. The research completed in this paper gathers a variety of information from different sources and attempts to apply it to a new situation. Some limitations of the current research are that the loading and boundary conditions used in the simulation have been based on previous models and have not been personally verified for accuracy. There is limited data on knee loading models and future work will be needed to completely verify the results generated by FEBio. Complete cadaver or anatomical subject testing would be needed to ensure that the results are accurate to predict the response to various loading conditions.

Also, the knee model used in the simulation was derived from a 70 year old woman who would have slightly different size knees than a man or other women. The dimensions and geometry for males and females may vary slightly, but this model is sufficient to extrapolate certain trends that may be seen in the data so that it can be applied to a larger population. While there are differences in the knees between subjects, the factors that most likely will influence the risk of injury are the weight of the person, the speed of the vehicles, and the angles of the legs just prior to impact. The current study will make some generalizations that may not apply to every person but the model should be sufficient for most.

The actual finite element model has several inherent limitations that may be addressed in further investigations. The Open Knee model did not include the joint capsule, patella, patellar tendon, or skin and these may have an effect on the reactions seen within the knee. The medial meniscus was not attached to the medial collateral

ligament or to the tibia along the periphery of the meniscus in the current model. Other limitations include inaccuracies in surface representations due to the manual construction of the 3D model and the low contrast magnetic resonance imaging used. The material properties used in the simulations were based on published literature and are not specific to the actual specimen. The ligament pre-strains were not defined in the model, possibly affecting the stress and strain. Although densities were assigned to each element, the femur and tibia were modeled as shell elements and do not accurately describe an actual femur or tibia. The simulations were run slowly which allows the density and inertia of the elements to be ignored but there could be some variation in the results if the densities were changed. While there are several limitations inherent in the current model, the results discussed here provide a good starting point for comparison and give approximate values for the loads required for meniscal injury.

4.2 Future Investigations

There is still work that can be done with this study to gain a more accurate and better understanding of the reactions within the medial meniscus when certain loads are applied to the knee. Additional validation of the materials, geometries, and boundary conditions are required to ensure the accuracy of the previously presented simulations. This can be done by using cadaver or anatomical testing to better determine the material characteristics and the reaction of the entire knee. Different geometrical knee models can be used to determine the effects of different sizes, such as comparing young male knee to an older female knee. It would also be beneficial to determine the effects of changing the settings used in the current analysis to validate the model. Further testing can be done to

see if changing settings, such as the density, time step size, and analysis type, will have a large effect on the simulation results. Once the model has been optimized and validated, the applied loads can be increased to higher values than those previously presented. This would give a better picture of the stresses and strains found within the meniscus instead of using extrapolation to determine them. Finally, a next step would be to determine if it is actually possible to produce these loading patterns in a rear end low-speed collision. This may be done with either actual test dummies, or by using other modeling software to find the reaction forces during a collision. The current work provides an excellent starting point to solve a significant problem, but future work is still needed to comprehensively validate the model and apply it to actual vehicle collisions.

5. Conclusion

The research presented here is the first study to determine the effects of applied compression and torques to the knee on the medial meniscus by using three-dimensional finite element analysis. It was shown that a variety of loads applied to the knee serve to increase the stress and strain within the medial meniscus and may increase them to a level that produces failure. Compressive loading in the direction of the long axis of the tibia with the knee in both the neutral and flexed positions increased the stresses and strains seen within the meniscus. With the knee in the neutral position, a compressive load greater than 1750 N may incur medial meniscal injury while increased knee flexion to 72 degrees can reduce the required compressive force to only 670 N. A compressive force coupled with either an axial or varus torque will increase the stress seen within the meniscus and will eventually create a tear as the material fatigues. If the knee is flexed to

72 degrees, axially loaded, and an axial torque is applied to the femur, the stress in the medial meniscus could increase by 35% while a varus torque could increase the stress by 25%. Either type of torque or flexion reduces the amount of compressive loading required to cause the same amount of stress within the medial meniscus. In a rear end, low-speed collision, there may be several scenarios that will create varying amounts of compressive loading or torque within the knee. A certain body position or magnitude of the collision could create a large amount of pure compression which would be sufficient to cause a tear in the meniscus, but if there is any movement of the knee that creates a torque, the compressive force required for injury would be significantly less. The results from the simulations discussed previously show that it is possible for the stress and strain levels within the medial meniscus to be elevated to levels that would cause a tear.

6. References

Anatomy of the Knee. (2001) Medical Internet Solutions. (http://www.aclsolutions.com/anatomy.php)

Bendjaballah, Shirazi-Adl, Zukor. (1995) Biomechanics of the human knee joint in compression: reconstruction, mesh generations and finite element analysis. *The Knee.* Vol. 2, No. 2. 69-79.

Bendjaballah, Shirazi-Adl, Zukor. (1997) Finite element analysis of human knee joint in varus-valgus. *Clinical Biomechanics.* Vol 12. No. 3. 139-148.

Bentley, G. (1996) Affections of the Knee Joint in Mercer's Orthopaedic Surgery. 9th Ed. London. Arnold. Chapter 16.

Bristow, W. R. (1925) Internal Derangement of the Knee Joint. *The Journal of Bone and Joint Surgery*. 7:413-450.

Bullough, P.G., Munuera, L., Murphy, J., Weinstein, A.M. (1970) The Strength of the Menisci of the Knee as it Relates to their Fine Structure. *The Journal of Bone and Joint Surgery.* Vol 52 B, No. 3: Pg 564-601.

Donahue, Hull, Rashid, Jacobs. (2002) A Finite Element Model of the Human Knee Joint for the Study of Tibio-Femoral Contact. *Journal of Biomechanical Engineering*. Vol. 124. Pg 273-280.

Donahue, Hull, Rashid, Jacobs. (2004) The sensitivity of tibiofemoral contact pressure to the size and shape of the lateral and medial menisci. *The Journal of Orthopedic Research.* 22, 807-814.

Erbagci, H., Gumusburun, E., Bayram, M., Karakurum, G., Sirikci, G. (2004) The normal menisci: in vivo MRI measurements. *Journal of Surgical and Radiologic Anatomy*. Vol. 26, No. 1.

Erdemir A., Sibole S. (2010) Open Knee: A Three Dimensional Finite Element Representation of the Knee Joint User's Guide, Version 1.0.0. Musculoskeletal Research Laboratory (MRL) (2010) The University of Utah, Salt Lake City, UT

Erskine, L.A. (1950) The Mechanisms Involved in Skiing Injuries. *American Journal of Surgery*. Volume 97. Pg. 667-671.

Fan, R.S.P., Ryu. R.K.N. (2000) Meniscal Lesions: Diagnosis and Treatment. *Medscape Orthopeadics & Sports Medicine.* 4(2).

Finite Element Theory. (2006) Chapter 2. pp 37-63. (http://www3.imperial.ac.uk/portal/pls/portallive/docs/1/1087902.PDF)

Frankel, Burstein, Brooks. (1971) Biomechanics of Internal Derangement of the Knee. *The Journal of Bone and Joint Surgery.* Vol. 53-A. No. 5.

Hauch, Villegas, Donahue. (2009) Geometry, time-dependent and failure properties of human meniscal attachments. *The Journal of Biomechanics.* 463-468.

Haut, T.L., Hull, M.L, Howell, T.S.M. (2000) Use of Roentgenography and Magnetic Resonance Imaging to Predict Meniscal Geometry Determined with a Three-dimensional Coordinate Digitizing System. *Journal of Orthopaedic Research*. 18:228-237.

Jayaraman, Sevensma, Haut. (2001) Effects of Anterior-Posterior Constraint on Injury Patterns in the Human Knee During Tibial-Femoral Joint Loading from Axial Forces through the Tibia. *Stapp Car Crash Journal*. Vol. 45, Pg 375.

Jury Verdict Review & Analysis (JVR&A). (2010) Verdict Search. (http://www.jvra.com/verdict_trak/professional.aspx? search=49).

Kennedy, J.C., Hawkins, R.J., Willis, R.B., Danylchuk, K.D. (1976) Tension Studies of Human Knee Ligaments. *The Journal of Bone and Joint Surgery.* Vol 58 A, No. 3.

Mansour, J. M. (2009) Biomechanics of Cartilage. *Biomechanical Principles*. Ch. 5. Pg 66-79.

Mathur, P.D., McDonald, J.R., Ghormley, R.K. (1949) A Study of the Tensile Strength of the Menisci of the Knee. *The Journal of Bone and Joint Surgery*. 1949;31:650-654.

National Highway Traffic Safety Administration (NHTSA) Vehicle Reports (2011)

Nordhoff, L. S. (2005) Motor Vehicle Collision Injuries. Biomechanics, Diagnosis, and Management. Jones and Bartlett Publishers, Inc.

Pena, E., Calvo, B., Martinez, M.A., Palanco, D., Doblare, M. (2005) Finite element analysis of the effect of meniscal tears and meniscectomies on human knee biomechanics. *Clinical Biomechanics*. 498–507.

Peterson, D.R., Bronzino, J.D. (2008) Biomechanics: Principles and Applications. Florida, CRC Press, Taylor & Francis Group.

Phisitkul, P., James, S.L., Wolf, B.R., Amendola. A. (2006) MCL Injuries of the Knee: Current Concepts Review. *The Iowa Orthopaedic Journal*. Vol. 26: 77-90.

Seedhom, Longton, Wright, Dowson. (1972) Dimensions of the knee: Radiographic and autopsy study of sizes required by a knee prosthesis. *Ann. Rheum. Dis.* 31(1): 54–58.

Shakespeare, Rigby. (1983) The Bucket Handle Tear of the Meniscus: A Clinical and Arthrographic Study. *The Journal of Bone and Joint Surgery.* Vol. 65-B. No. 4.

Solomen, Simel, Bates, Katz, Schaffer. (2001) Does This Patient Have a Torn Meniscus or Ligament of the Knee? Value of the Physical Examination. *The Rational Clinical Examination*. Vol. 286, No. 13. Pg 1610-1620.

Stone, Freyer, Turek, Walgenbach, Wadhwa, Crues. (2007) Meniscal Sizing Based on Gender, Height, and Weight. *The Journal of Arthroscopic and Related Surgery.* Vol 23, No 5, pp 503-508.

Tichon, D.J., Peterson, D.R. (2011) Effect of Rear End Low-Speed Collisions on the Meniscus. *Northeast Bioengineering Conference*. Poster Presentation.

Tissakht, M., Ahmed, A.M. (1995) Tensile Stress-Strain Characteristics of the Human Meniscal Material. *Journal of Biomechanics*. Vol. 28, No. 4, pp 411-422.

WebMD. (2009) Meniscus Injuries. (http://emedicine.medscape.com/article/90661-overview).

Yoshioka, Siu, Cooke. (1987) The anatomy and functional axes of the femur. *The Journal of Bone and Joint Surgery*. 69:873-880.

7. Appendix A- Motor Vehicle Knee Injury Statistics

1. Summary of Motor Vehicle Knee Injury Statistics (JVR&A, 2010)

	Cases Found	**Percentage**	
Total Motor Vehicle Negligence Cases	40728		
Total Rear End Collisions	11614	29%	of all motor vehicle cases
Total Rear End Collision Knee Injuries	720	6.2%	of rear end collisions
Meniscus Tears	178	25%	of knee injuries
		2%	of rear end collisions
Medial Meniscus Tears	81	46%	of meniscus tears
Lateral Meniscus Tears	13	7.3%	of meniscus tears
Unknown Meniscus Tears	84	47%	of meniscus tears
ACL Tears	26	3.6%	of knee injuries
		0.2%	of rear end collisions
PCL Injury	3	0.4%	of knee injuries
		0.03%	of rear end collisions
MCL Injury	2	0.3%	of knee injuries
		0.02%	of rear end collisions
LCL Injury	1	0.1%	of knee injuries
		0.01%	of rear end collisions
Chondromalacia Patella	11	1.5%	of knee injuries
		0.1%	of rear end collisions
Patella Fracture	14	1.9%	of knee injuries
		0.1%	of rear end collisions
Femur Fracture	28	3.9%	of knee injuries
		0.2%	of rear end collisions
Tibia Fracture	35	4.9%	of knee injuries
		0.3%	of rear end collisions
Unknown Knee Injuries	422	59%	of knee injuries
		3.6%	of rear end collisions

2. Summary of Rear End Collisions Involving Knee Injury (JVR&A, 2010)

No.	Age	Gender	Driver?	Crash Type	Target/Bullet	Comments
1	47	M	Y		T	
2	30	F	Y		T	medial
3	43	F	Y	stopped	T	patello-femoral syndrome
4	55	F	rear	stopped	T	medial
5	30s	M	Y	moving	T	
6	19	M	Y	moving	T	no seatbelt
7		M			T	medial
8	38	F	Y	moving	T	flipped on side, dashboard contact
9		M	Y	moving	T	medial, previous injuries
10	28	F				
11	45	F	Y	moving	T	horizontal tear
12	73	F	Y	fast moving	T	torn meniscus + fractured tibia
13	30s	M	Y	stopped	T	dashboard contact
14	50	M	Y	stopped	T	medial
15		M	Y	slow moving	T	dashboard contact
16		F	Y	stopped	T	
17	50s	M	Y	stopped	T	medial, dashboard contact
18	49	M	Y	stopped	T	bilateral
19		M	Y	stopped	T	2 tears
20	68	F	Y		T	dashboard contact
21	60s	F	Y	moving	T	medial, dashboard contact
22		M	N	hit truck	B	bus passenger
23	20s	M	Y			
24	60s	F			T	medial
25	41	M	Y	moving	T	medial, dashboard contact
26	20	F	N		T	knee cap fracture, dashboard contact
27	38	F	Y	stopped	T	morbidly obese
28	50	M	Y		T	medial posterior horn
29	24	F				
30	70s	F	Y	stopped	T	
AVG	45	15M / 15F	13 Y			

8. Appendix B- Physical and Material Properties of the Meniscus

1. Compiled Dimensions of Bony Aspects of Femur (Seedhom et al, 1972); (Yoshioka et al, 1987)

	Reference 26		Reference 27		Average	
	Male	**Female**	**Male**	**Female**	**Male**	**Female**
Max Width of Femoral Condyles (mm)	80	74	83	72	81.5	73
Width of Lateral Condyle (mm)	29.52	28.19	31	28	30.26	28.095
Width of Intracondylar Notch (mm)	21.84	17.69	13	11	17.42	14.345
Width of Medial Condyle (mm)	28.4	12.25	32	27	30.2	19.625

2. Cross Sectional Dimensions of Meniscus (Erbagci et al, 2004)

	Height (mm)	**Width (mm)**	**Area (mm^2)**
Medial Meniscus			
anterior horn	5.32	7.78	41.3896
mid-body	5.03	7.37	37.0711
posterior horn	5.53	11.71	64.7563
Lateral Meniscus			
anterior horn	4.33	8.88	38.4504
mid-body	4.94	8.37	41.3478
posterior horn	5.36	9.7	51.992

3. Overall Dimensions of Meniscus (Hauch et al, 2009)

	<25 BMI	**>25 BMI**	**Average**
Lateral meniscus width (cm)	2.84	2.98	2.91
Lateral meniscus length (cm)	3.48	3.7	3.59
Medial meniscus width (cm)	2.95	3.22	3.09
Medial meniscus length (cm)	4.38	4.51	4.45
Total tibial plateau width (cm)	7.37	7.84	7.61

4. Transverse and Cross Sectional Dimensions of Medial Meniscus (Stone et al, 2007)

	Mean (mm)	Min (mm)	Max (mm)
Depth	37.99	30.62	44.08
Width-ant	23.60	17.00	29.00
Width-post	25.10	21.50	29.50
w-ant	10.61	6.75	17.83
w-mid	11.93	7.09	15.13
w-post	14.65	9.31	19.78
h-ant	6.62	4.11	8.67
h-mid	7.08	4.26	10.33
h-post	6.01	4.10	7.50
b-ant	0.15	-0.43	0.87
b-mid	-0.24	-1.82	0.24
b-post	0.20	-1.19	1.54
h/h_o -ant	1.58	1.07	2.85
h/h_o -mid	1.49	1.07	1.94
h/h_o -post	2.40	1.08	9.30
h_o/w_o -ant	25.28	15.77	35.00
h_o/w_o -mid	23.48	19.47	28.40
h_o/w_o -post	15.49	4.45	21.60

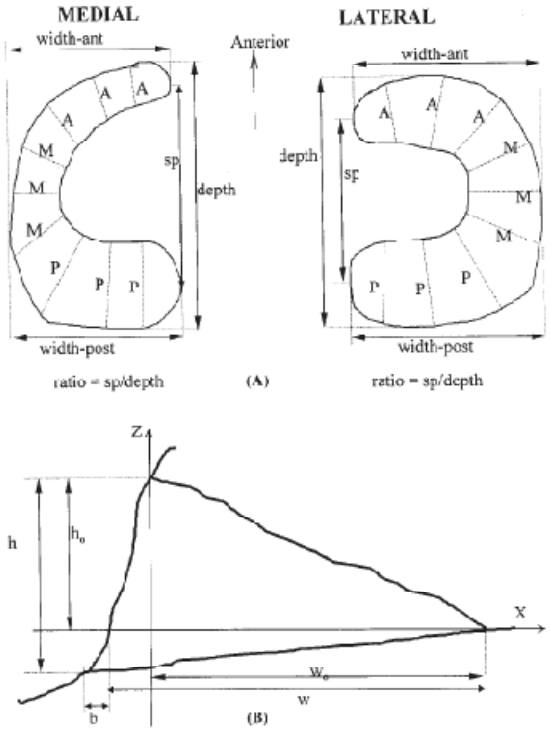

5. Material Properties of the Bones set in FEBio (Erdemir et al, 2010)

Bone	Density (tones/mm^3)
Femur	1.132e-6
Tibia	1.132e-6

6. Material Properties of the Ligaments set in FEBio (Erdemir et al, 2010)

Ligament	Density	C_1	C_2	K	C_3	C_4	C_5	λ_m
ACL	1.5e-9	1.95	0	73.2	0.0139	116.22	535.039	1.046
PCL	1.5e-9	3.25	0	122	0.1196	87.178	431.063	1.035
MCL	1.5e-9	1.44	0	397	0.57	48	467.1	1.063
LCL	1.5e-9	1.44	0	397	0.57	48	467.1	1.063

7. Material Properties of the Cartilages set in FEBio (Erdemir et al, 2010)

Density	C_1	C_2	K
1.5e-9	0.856	0	8